Journal of Materials Chemistry A

ROYAL SOCIETY OF CHEMISTRY

REVIEW

View Article Online
View Journal | View Issue

Cite this: J. Mater. Chem. A, 2026, 14, 2011

A comprehensive and critical review on the application of conductive polymers as coatings for aqueous zinc-ion battery positive electrode materials

Mohsen Baghodrat,[a] Fabio La Mantia *[ab] and Giorgia Zampardi *[a]

Aqueous zinc-ion batteries (A-ZIBs) offer advantages in terms of cost, safety, and eco-friendliness. However, their commercialization has been hindered by challenges such as limited cycle life and suboptimal capacity, mainly arising from the properties of their positive electrode materials. This review provides a detailed assessment of the incorporation of conductive polymers, namely poly(3,4-ethylenedioxythiophene) (PEDOT), polypyrrole (PPy), and polyaniline (PANI), to improve the electrochemical properties of common positive electrode materials in A-ZIBs. Ranging from expanding the interlayer spacing in vanadium oxides to mitigating the dissolution of manganese in manganese oxides, and extending the cycle life of Prussian blue analogues, conductive polymers present a promising avenue for the next generation of aqueous zinc-ion batteries. By offering a comprehensive evaluation of the recent studies in this field, we aim to clarify the current state of the research, draw attention to potential misinterpretations, and spotlight the potentials for future exploration.

Received 23rd July 2025
Accepted 30th November 2025

DOI: 10.1039/d5ta05963a

rsc.li/materials-a

1. Introduction

As the demand for green, sustainable, and efficient energy storage solutions grows, advanced battery technology has become a critical area of focus. Lithium-ion batteries (LIBs) have traditionally been the most prominent battery technology, serving a diverse array of applications from portable electronics to electric vehicles. However, the challenges related to cost, safety, and the limited availability of lithium resources have necessitated the exploration of alternative battery chemistries.[1–3] In this context, aqueous zinc-ion batteries (A-ZIBs) stand out as a viable alternative thanks to their numerous benefits, including high energy density, inherent safety offered by the aqueous electrolyte, and the abundant, cost-effective, and eco-friendly nature of zinc.[4–6] Such attributes directly address the issues typically associated with organic-based battery systems, primarily lithium-ion batteries.

Despite their advantageous characteristics, the practical implementation of A-ZIBs has been impeded by several difficulties, notably the hydrogen evolution at the negative electrode (often referred to as "anode")[7–9] and a limited choice of suitable positive electrode active materials (often referred to as "cathode").[6,10–12] The ideal positive electrode active material should possess several key attributes, including high capacity, high rate-capability, satisfactory conductivity, low toxicity, synthesis easily scalable at the industrial level, and durable structural stability over prolonged cycling.

The most commonly studied positive electrode active materials in A-ZIBs include manganese oxides (MnO_2 or Mn_2O_3), vanadium oxide (V_2O_5), and Prussian blue analogs (PBAs), each with their own advantages and limitations.[10,12] Manganese oxide-based positive electrodes offer cost-effective and eco-friendly properties, coupled with diverse crystal structures that facilitate the (de-)intercalation of Zn^{2+}. Nevertheless, they suffer from poor electrical conductivity, severe capacity fading, and limited cycle life, primarily attributed to the irreversible dissolution of manganese into the electrolyte.[13–16] V_2O_5 boasts a high theoretical capacity and can facilitate the insertion of Zn^{2+} owing to its tunnel-like structure. However, it also suffers from sluggish kinetics, poor cycle life, and especially low Zn insertion potential that ultimately reduces the energy density of the final Zn-ion cell.[13,17–19] Other potential candidates as active materials for the positive electrodes of A-ZIBs can be found within the family of Prussian blue analogues. PBAs are defined by the nominal formula of $A_xM_1[M_2(CN)_6]_z \cdot wH_2O$, where A symbolizes an alkali metal, and M_1 and M_2 represent transition metal elements. With their unique open-framework structure, they can facilitate the storage of Zn^{2+} and have shown promising results in terms of power density and rate capability.[20] Furthermore, they usually exhibit high Zn-insertion potentials, are cost-effective, and their synthesis can be easily scaled up.

[a]Universität Bremen, Energiespeicher- und Energiewandlersysteme, Bibliothekstraße 1, 28359 Bremen, Germany. E-mail: lamantia@uni-bremen.de; zampardi@uni-bremen.de
[b]Fraunhofer Institute for Manufacturing Technology and Advanced Materials – IFAM, Wiener Straße 12, 28359 Bremen, Germany

However, crystal structure of PBAs suffers from irreversible phase transformations after the continuous Zn^{2+} (de-)insertion, detrimentally affecting their cycle life.[20–22]

All these challenges associated with the current positive electrode active materials represent a significant bottleneck in the commercialization of A-ZIBs. Therefore, there is a pressing need to explore novel materials or innovative modifications to the existing ones to fully leverage their potential.

A promising strategy that started gaining interest in the scientific community, as demonstrated by the trend of the number of publications summarized in Fig. 1, to overcome these challenges lies in the utilization of composite or coated electrodes, constructed from conductive polymers and Zn^{2+} intercalating materials. Conductive polymers, with their high conductivity and flexibility, offer a potentially viable solution to issues encountered by conventional Zn^{2+} storage materials. While alternative conductive materials such as carbon supports (*e.g.*, graphene, carbon nanotubes, and carbon black) improve the electrical conductivity and can provide porous frameworks, they fail to effectively suppress transition-metal dissolution. Similarly, metallic additives like silver can enhance the electrical conductivity but raise greatly the costs and pose corrosion risks in aqueous electrolytes. In contrast, conductive polymers maintain the structural integrity of the active material, protect it from undesirable side reactions, buffer its volume changes resulting from repeated Zn^{2+} (de-)intercalation, and decrease the active material dissolution, while enhancing the overall conductivity of the electrode.[13,17]

Conductive polymers have been employed in many components of A-ZIBs, including negative electrodes (often referred to as "anodes"), positive electrodes (often referred to as "cathodes"), separators, and electrolytes. Whereas previous reviews surveyed this broad landscape or focused on early composites,[13,23] our work will focus exclusively on the use of conductive polymers in the positive electrode side of an aqueous Zn-ion battery. By narrowing the scope to the positive electrodes, we will explore how polymer chemistry and architecture can influence the Zn^{2+} intercalation processes and affect the aging of the active materials.

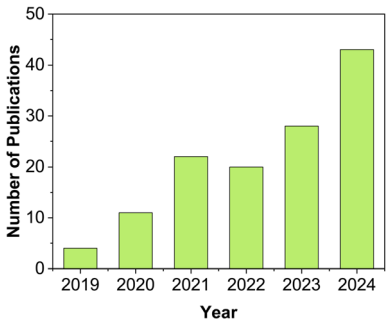

Fig. 1 Number of total scientific publications per year of the reported literature using conductive polymer coatings/composites as a strategy to improve the performance of aqueous Zn-ion batteries. Data collected in March 2025 from Clarivate Web of Science. Keywords used: "aqueous zinc-ion batteries", "PEDOT", "PEDOT:PSS", "PPy", "PANI".

This review aims to offer a comprehensive and critical evaluation of the recent research studies on the merits of integrating conductive polymers in positive electrodes for A-ZIBs, identifying potential misinterpretations, and highlighting potential areas for future investigation. Moreover, we will attempt to re-benchmark the published experimental data and performance using application-relevant metrics (*e.g.*, mass loading, areal capacity, actual C-rate, *etc.*), which has not been systematically discussed in earlier surveys. Last but not the least, we will emphasize mechanistic insights and standardization challenges, highlighting the limitations in current laboratory testing, and proposing realistic testing conditions.

2. Common conductive polymers for A-ZIBs

The most commonly studied conductive polymers in the frame of aqueous Zn-ion batteries include poly(3,4-ethylenedioxythiophene) (PEDOT) and/or its blend with polystyrene sulfonate (PSS) abbreviated as PEDOT:PSS, polypyrrole (PPy) and polyaniline (PANI). The commonality among these polymers is the alternating of single and double bonds along the backbone of the polymer, forming a so-called conjugated system. Each carbon atom of the polymer chain is in fact capable of forming four bonds, but in the case of the carbon atoms present in the conductive polymers' backbone, three of these bonds are already used to form a bond with the adjacent atoms in the backbone, leaving the fourth bond as a π-bond. These free π-bonds of the carbon atoms overlap and delocalize along the entire polymer chain, allowing for electrical conduction. This unique property of conductive polymers enabled them to be utilized in a wide range of applications, such as solar cells,[24,25] sensors,[26–28] anti-corrosive coatings,[25,29] and batteries.[13,30,31]

The choice of PPy, PANI, PEDOT, and PEDOT:PSS over other polymers for applications in A-ZIBs can be justified based on several factors. Their high electrical conductivity and electrochemical performance is crucial to meet the specific electrical requirements of A-ZIBs. Moreover, these polymers do not react adversely when in presence with Zn^{2+} ions, the aqueous electrolyte and the elements of common A-ZIB cathode materials, thus their electrochemical stability ensures high efficiency and lifespan of the electrodes and facilitates their application in A-ZIBs. Moreover, the synthesis routes and processing methods of PPy, PANI, and PEDOT are well-established, making them readily applicable to battery research. These materials can be easily deposited onto various substrates using techniques such as electrodeposition and chemical oxidative polymerization.[13]

2.1 PEDOT and PEDOT:PSS

The structure of the ethylenedioxythiophene (EDOT) monomer, which forms the repeating unit in the PEDOT chain (Fig. 2), is essentially constituted by a thiophene ring with two additional carbon atoms bridging the 3 and 4 positions of the ring through an oxygen atom. In its doped state, PEDOT is known for having one of the highest conductivity levels among all conductive

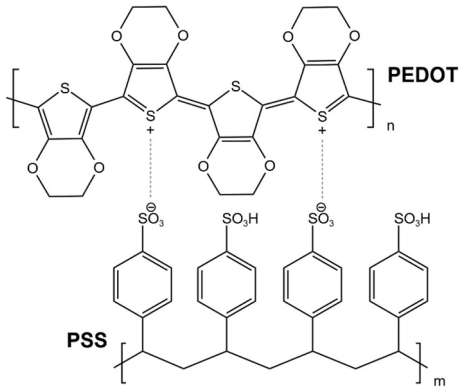

Fig. 2 Chemical structure of PEDOT:PSS.

polymers.[32] However, its electrochemical stability in aqueous electrolytes is still debated among researchers.[26,33–36] Experimental evidence suggests that PEDOT undergoes over-oxidation in acidic electrolytes at potentials exceeding 1 V *vs.* RHE, triggering a rapid degradation of the material.[33,34] Such conditions could potentially constrain the use of PEDOT in A-ZIBs, where these potentials coincide with the upper bounds of the cycling voltage window (≥1.7 V *vs.* Zn^{2+}/Zn). Furthermore, the processability of PEDOT is hampered by its difficult dispersion in many common solvents, notably in water. To surmount these limitations, a blend of PEDOT with PSS, designated as PEDOT:PSS and depicted in Fig. 2, has been proposed.[37] This blend harnesses the beneficial properties of PSS to enhance the electrochemical stability, processability, and dispersibility in water of PEDOT, thus facilitating its deployment in various water-based environmentally friendly applications. Moreover, PEDOT:PSS is proven to be thermally stable up to around 160 °C; however, its thermal stability depends on various parameters such as the addition of co-solvents (*e.g.* DMSO) and the PEDOT to PSS ratio.[38,39]

Commercial PEDOT:PSS (Clevios™, PH1000) is known for having one of the highest conductivity levels among all conducting polymers, which can reach 1000 S cm^{-1} after the addition of co-solvents.[39] However, PEDOT:PSS also has its challenges. For example, although it is water-processable, it is hygroscopic as well, meaning it readily absorbs water molecules from the environment, which can affect its performance over prolonged storage.[40,41] Furthermore, the PSS component, although it aids in terms of processability, does not contribute to the electronic conductivity. Therefore, methods are often employed to balance the PEDOT and PSS content to optimize the properties of the final PEDOT:PSS films.[39] Lastly, the electronic conductivity can be increased by several orders of magnitude through various treatment methods such as adding high boiling solvents, acid treatment, or thermal annealing.[38,42]

We believe that in addition to the unique properties of PEDOT:PSS in comparison to the bare PEDOT as mentioned before, one further advantage is the ease of use of PEDOT:PSS during the preparation of the composite or coated electrodes having as active materials the ones usually employed in A-ZIBs. Commercial PEDOT:PSS in the form of a stable dispersion in water can be mixed easily at room temperature with the cathode active materials, bringing even better electrochemical properties than the materials prepared with the bare PEDOT.[43,44]

2.2 PPy

The exploration of polypyrrole (PPy) dates back to significant early research, with Weiss *et al.*[45–47] achieving a form of PPy through the pyrolysis of tetraiodopyrrole in 1963. However, its notable conductivity was explicitly demonstrated in 1980,[48,49] marking the beginning of its exploration as a conductive polymer.

The PPy chain consists of repeating units of pyrrole, which are five-membered heterocyclic rings composed of four carbon atoms and one nitrogen atom (Fig. 3). PPy can be deposited from aqueous solutions onto various substrates by a number of techniques, such as electrodeposition[50–52] and chemical oxidative polymerization.[53,54] Two common oxidizing agents are ammonium persulfate, $(NH_4)_2S_2O_8$,[54] and ferric chloride, $FeCl_3$.[55]

Like many conductive polymers, the electrical properties of PPy can be adjusted by doping the chain with foreign atoms to increase the number of charge carriers.[56] Lastly, PPy films exhibiting a high electronic conductivity, exceeding 500 S cm^{-1}, can be prepared by choosing the appropriate polymerization conditions.[57]

The simple synthesis process of PPy, its biocompatibility, environmental stability, low-cost fabrication, and impressive conductivity have led to widespread use in electronics, energy storage, and biomedical applications.[13]

2.3 PANI

Polyaniline (PANI) traces its origins to the nineteenth century, discovered by Letheby, who observed the formation of a green substance after the electrochemical and chemical oxidation of aniline. This substance, later identified as PANI, has been extensively explored for its light weight, flexibility, and electrical conductivity.

The distinct physical and chemical properties of PANI allowed its wide application in a variety of fields, such as sensors, rechargeable batteries, and corrosion protection.[58,59] Both chemical and electrochemical polymerization methods can be utilized to synthesize PANI from aniline monomers. The distinguishing feature of PANI lies in its structural versatility, which enables it to exist in several oxidation states. The electrical conductivity of PANI depends primarily on its oxidation state and the type and degree of doping and protonation. The

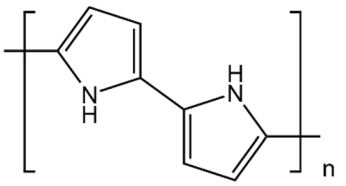

Fig. 3 Chemical structure of polypyrrole.

conductivity ranges from an insulating state to a highly conductive state of 10–200 S cm^{-1}.[60] The completely reduced form of PANI (leucoemeraldine) contains only benzenoid rings, and the fully oxidized form (pernigraniline) contains quinonoid rings as repeating units. The half-oxidized form of PANI, containing both benzenoid and quinonoid rings, is called emeraldine. These three forms of PANI can become conductive upon subsequent reduction or oxidation and protonation in an acidic environment, as depicted in Fig. 4. These processes ultimately result in the emeraldine salt form of PANI, in which the polymeric chain consists of alternating nitrogen atoms carrying a positive charge balanced by an anion. This protonated form is conductive due to the movement of the positive charges along the polymer backbone.

Table 1 summarizes the advantages and the disadvantages of PEDOT, PPy, and PANI.

3. Use of conductive polymers in A-ZIBs

3.1 A-ZIBs based on vanadium oxides

The focus of most studies on enhancing the electrochemical performance of vanadium oxides-based A-ZIBs has primarily revolved around strategies to enlarge the interlayer spacing of the vanadium oxide lattice.[13,17] An increased spacing would allow for the accommodation of more Zn^{2+} ions and promote a faster Zn^{2+} (de-)intercalation, thereby resulting in an enhanced capacity and an improved rate capability. Common approaches to adjust the interlayer spacing of vanadium oxides include inserting various metal guest ions (such as Li^+, Na^+, K^+, Mg^{2+}, Ni^{2+} and Al^{3+}) in the lattice.[61,62] Despite the efforts, this method is often constrained to less than 13 Å of enlarged interlayer distance, and sometimes a faster disintegration of the material's structure is reported over repeated charge/discharge cycles.[61,62]

A new strategy to enlarge interlayer spacing has emerged through a series of recent studies suggesting the incorporation of conductive polymers into vanadium oxides (Fig. 5). Taking V_2O_5 – the most commonly studied type among the vanadium oxides in A-ZIBs – as an example, literature shows that the incorporation of conductive polymers results in an enlarged interlayer distance and a reduced strain and stress within the V_2O_5 structure. Fig. 5 schematically illustrates a PPy-intercalated V_2O_5 layered material and how PPy chains expand the interlayer spacing of V_2O_5. This process is accompanied by an increase in the V^{4+}-to-V^{5+} ratio within the lattice due to charge compensation. This charge compensation also triggers the creation of oxygen vacancies within the lattice, leading to improved ionic diffusion, enhanced conductivity of layered oxides, and easier Zn^{2+} (de-)intercalation.[63–69] As shown in Fig. 6, Density Functional Theory (DFT) studies highlight how the incorporation of a polymer into V_2O_5 could modify the electron distribution around the active material. The polymer intercalation may result in a shielding effect weakening the electrostatic interactions between the Zn^{2+} ions and the host lattice, thereby enhancing the ionic diffusion kinetics.[68,70] Moreover, as demonstrated in Fig. 7, several studies show that the long initial activation of the redox sites, which is common for V_2O_5-based electrodes, vanishes or shortens when conductive polymers are introduced in the material's lattice.[66,71,72] This is attributed to a facilitated access of the Zn^{2+} ions to the redox sites thanks to the highly conductive network offered by the polymer molecules.[66,71,72] Interlayer spacing modifications in the structure of V_2O_5 are also linked with an elevated discharge capacity, better long-term cycling stability, and enhanced rate capability.

An increased interlayer spacing of the V_2O_5 from 4.38 to 13.95 Å has been reported using PEDOT in the works of Li and coworkers.[72] They prepared a positive PEDOT-intercalated V_2O_5-based electrode with improved structural stability. Their electrochemical characterizations performed in a 3 M $Zn(CF_3SO_3)_2$ aqueous solution showed an initial discharge capacity of 370.5 mAh g^{-1} at 0.5 A g^{-1} that reached 303.1 mAh g^{-1} after 100 cycles. On the other side, a bare V_2O_5 electrode without the addition of PEDOT reached a lower specific capacity of 233 mAh g^{-1} after 100 cycles under the same cycling conditions.

Using PPy, both Feng *et al.*[73] and Wang *et al.*[67] adopted a similar approach and observed that the presence of PPy successfully increased the interlayer spacing of their vanadium

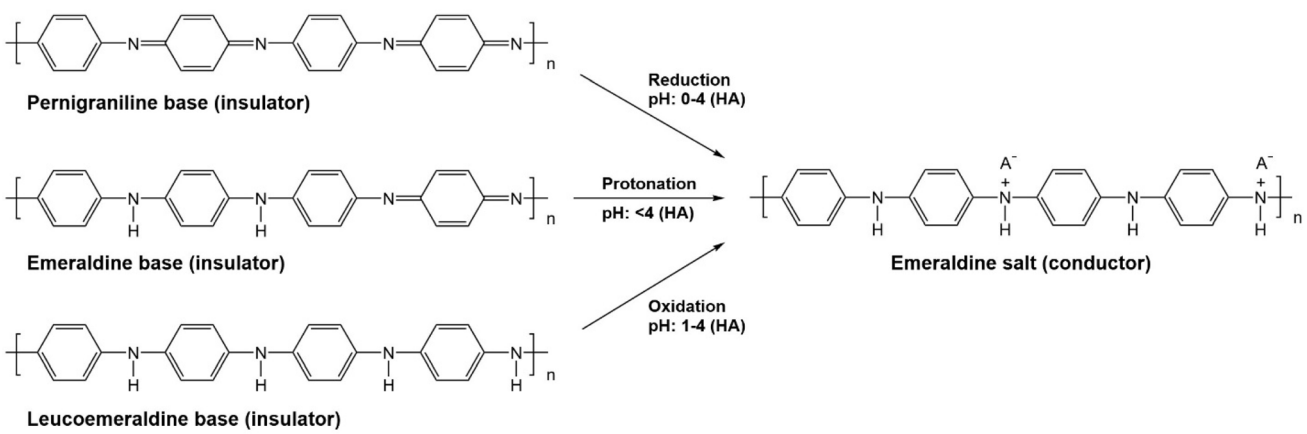

Fig. 4 Synthetic scheme of PANI in emeraldine salt form.

Table 1 Summary of the monomer constituting the different polymers used in the field of aqueous ZIBs, highlighting prices, advantages and disadvantages

Polymer	Monomer	Price of the monomer (€ per kg)	Advantages[a]	Disadvantages
PEDOT	EDOT	950	• Good thermal stability	• Electrochemical instability in acidic solutions at potentials ≥ 1.7 V *vs.* Zn^{2+}/Zn
			• Relatively high conductivity	• Difficult dispersion in many common solvents
				• Relatively high monomer cost
PEDOT:PSS	EDOT	950	• Easy processability	• Hygroscopic nature may affect its long-term stability
	PSS	600	• Commercially available	• Relatively high monomers costs
	Clevios PH100	500	• Very high conductivity up to 1000 S cm^{-1}	
PPy	Py	300	• Well-established and diverse synthesis routes	• Poor mechanical properties
			• Relatively biodegradable	• Homogeneous PPy layers with uniform structure difficult to obtain
			• Relatively biocompatible	• Difficult electropolymerization
PANI	ANI	75	• Tunable electrochemical properties	• Relatively low conductivity
			• Easy synthesis routes	• High toxicity of the monomer to both aquatic life and human health

[a] The conductivity of conductive polymers is heavily affected by their synthesis route, application environment, and presence of additives, co-polymers and/or co-solvents, their physical state, doping agents and doping level.

oxide up to 14.8 Å, leading to improved specific discharge capacity of 325 mAh g^{-1} at 0.5 A g^{-1}. Moreover, it has been shown that introducing pyridinesulfonic acid (PSA) in the synthesis process of the PPy-intercalated V_2O_5 can lead to even larger interlayer spacings.[62] In this case, the nitrogen-containing groups in PSA is supposed to interact with vanadium to further expand the interlayer spacing of V_2O_5, and the sulfonic groups facilitate the polymerization of PPy, leading to an even larger interlayer spacing of up to 15.8 Å (ref. 62) (Fig. 8).

Increasing further the interlayer distance to 29 Å obtained through the use of PEDOT:PSS,[65] an initial discharge capacity of 400 mAh g^{-1} at 0.5 A g^{-1} has been reported. This hydrothermally synthesized PEDOT–PSS-intercalated V_2O_5 maintained 89.4% of discharge capacity after 2000 cycles rated at 5 A g^{-1}. Comparatively, the bare V_2O_5 maintained only 50.9% of capacity under the same conditions.

In a few studies on PANI-intercalation in V_2O_5, a unique flower-like microstructure has resulted after introducing the polymer. This structure is in contrast with the commonly seen 2D belt-like or sheet-like architectures. It has been suggested that the construction of 3D structures may result in faster Zn^{2+} diffusion kinetics as well as in a more durable structural

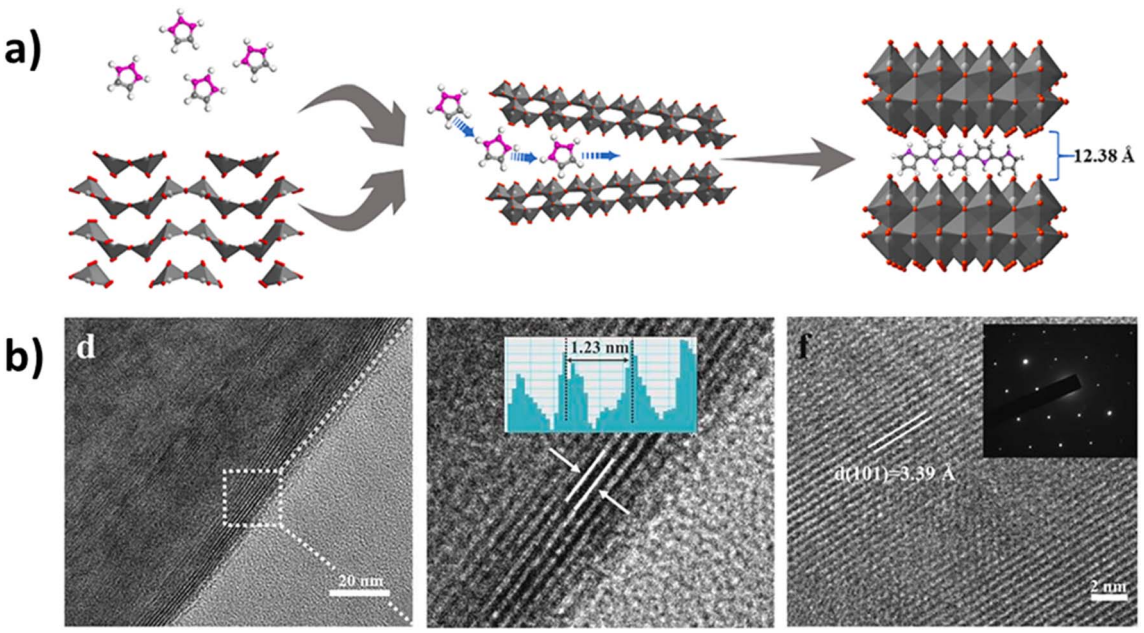

Fig. 5 (a) Schematic illustration of the preparation process of PPy-intercalation V_2O_5 layered material. (b) HRTEM images of as-prepared PPy-V-10 sample. Reprinted from ref. 67, copyright (2022), with permission from Elsevier.

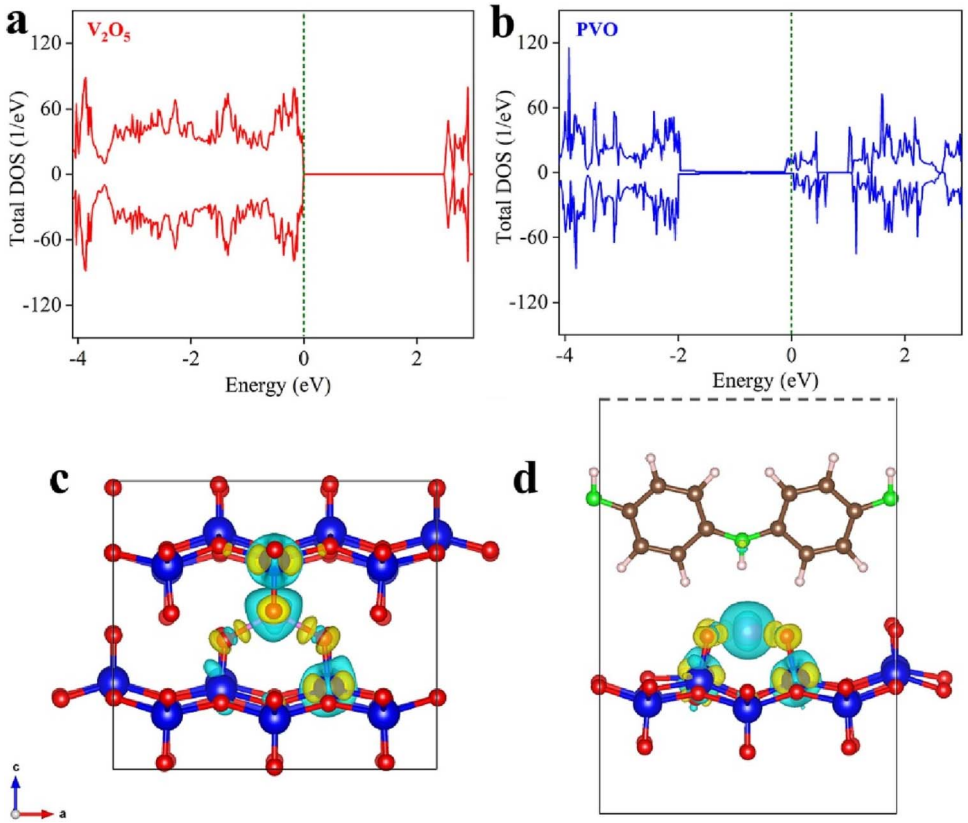

Fig. 6 Total density of states for (a) pristine V_2O_5 and (b) PVO (V-MOF-derived hierarchical porous V_2O_5). (c and d) Differential charge density with Zn^{2+} intercalation in V_2O_5 and PVO. Color code: blue, red, brown, green, purple, and white balls represent V, O, C, N, Zn, and H atoms, respectively. Reprinted from ref. 68, copyright (2023), with permission from Elsevier.

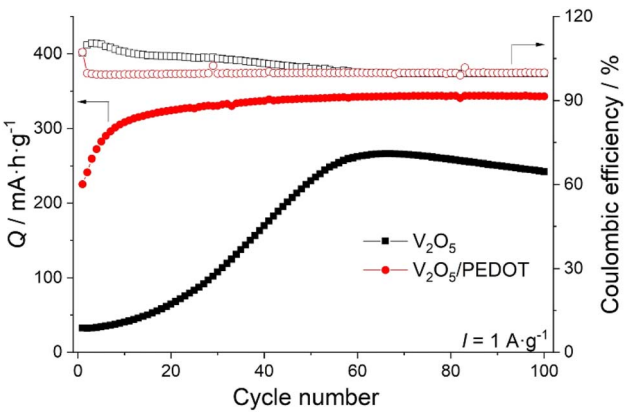

Fig. 7 Electrochemical performance of V_2O_5 and V_2O_5/PEDOT electrodes: cycle performance at 1 A g^{-1}. Reprinted from ref. 66, copyright (2022), with permission from Elsevier.

reversibility. Sun *et al.*[74] showed that the intercalation of PANI into layered vanadium oxide leads to improved charge storage capacity and cycling stability. More specifically, it led to a high specific discharge capacity of 325 mAh g^{-1} at 0.5 A g^{-1} and a good cycling stability with 92% capacity retention after 3000 cycles at 1 A g^{-1}.

Polymer-intercalated vanadium oxide is typically synthesized through the hydrothermal method by mixing vanadium oxide with the monomers in an autoclave under controlled pH, temperature, and time. However, alternative methods are emerging, offering lower energy demand or more environmentally friendly approaches. For instance, as illustrated in Fig. 9, PEDOT-intercalated V_2O_5 may be prepared using an aerogel made out of a V_2O_5 ink and EDOT monomers after gelation and freeze drying and eventually mixed with carbon nanotubes.[64] Furthermore, carrying out microwave-induced polymerization is another alternative synthesis method as described in ref. 66.

The interface-intercalation method is another approach that Zhang *et al.* utilized.[61] In this case (Fig. 10), V_2O_5 hydrogel aqueous dispersion is introduced to an organic mixture of aniline monomers and CCl_4. The resulting material, PANI-hydrated vanadium oxide, demonstrated a better electrochemical performance due to its 3D sponge-like morphology, high surface area (190 m^2 g^{-1}), and expanded interlayer spacing (14.1 Å). The construction of the 3D structure resulted in faster Zn^{2+} diffusion kinetics as well as more durable structural reversibility. This structure enabled an approximate 60% increase in discharge capacity (360 mAh g^{-1} at 0.1 A g^{-1}), however allowed only a limited capacity retention of 80% in *ca.* 30 cycles.

Conductive polymers can also be used as coatings on the surface of the active materials rather than diffusing in the

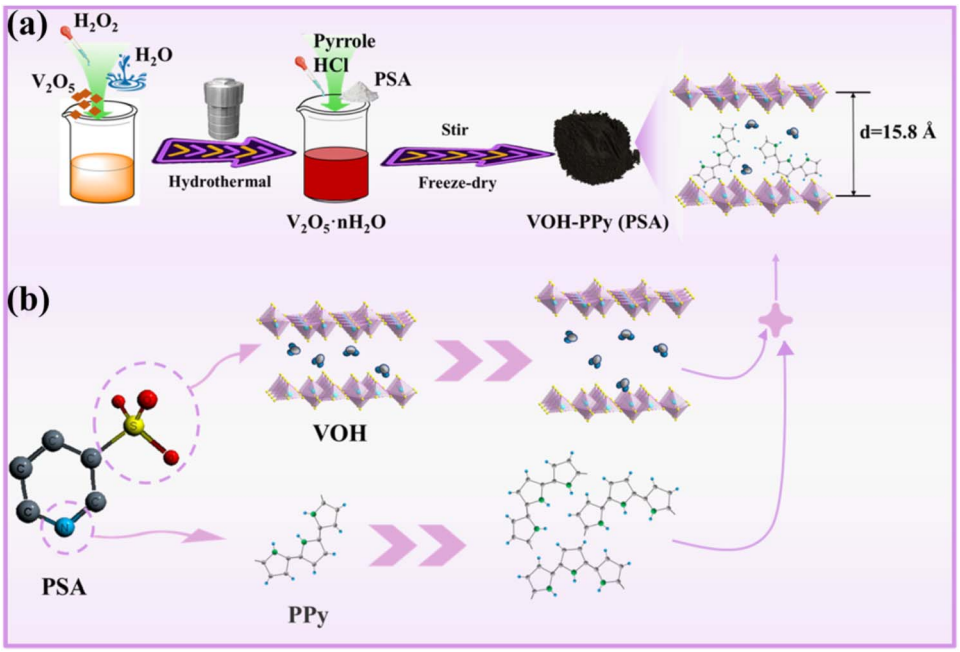

Fig. 8 (a) Schematic illustration of the fabrication of hydrated-V_2O_5–PPy (VOH–PPy) in an acidic environment with PSA added (denoted as VOH–PPy (PSA)) and (b) description of PSA's role. Reprinted from ref. 62, copyright (2021), with permission from ACS.

interlayer spaces of their lattice. This method offers an alternative way to strengthen the structural stability and prolong the cycle life of the cathodes. For instance, Zhang *et al.*[63] utilized this polymerization strategy to prepare PPy-coated V_2O_5 nanobelts at room temperature. During this process, V_2O_5 plays the role of an oxidation agent for polymerization. This approach contributed to a *ca.* 60% decrease in the charge transfer resistance and to achieve a specific capacity retention of 95.92% after 2000 cycles at a very high current density of 5 A g^{-1}. Following a similar method, it has been showed[69] that coating PANI on V_2O_5 nanobelts resulted in a core–shell structure (Fig. 11) with a 40% improved specific capacity (270 mAh g^{-1} at a low current density of 0.5 A g^{-1}) and a capacity retention of 98% after 2000 cycles at 2 A g^{-1}.

To further improve the performance of vanadium-based A-ZIBs, conductive polymers can be coupled with more novel Zn^{2+} intercalating materials. In a study by Kumankuma-Sarpong *et al.*,[71] PEDOT was incorporated within yttrium-vanadium oxide (PEDOT@YVO), synthesized *via* hydrothermal oxidation polymerization of EDOT mixed with YVO. Their findings highlighted the long-term durability of PEDOT@YTO and the role of PEDOT in enlarging the interlayer distance, facilitating the Zn^{2+} diffusion, shortening the ion-diffusion paths, lowering the electron transport resistance, and improving the electrical conductivity. The electrochemical parameters of their composite electrodes have been measured by cycling at a current rate of 1C, following the envisaged standard rates for the application of A-ZIBs. As depicted in Fig. 12, bare YVO showed continuous deterioration in aqueous 2 M $Zn(CF_3SO_3)_2$, namely 30.6% of capacity retention after 2500 cycles. Comparatively, the PEDOT@YVO electrode delivered a higher stability, reaching 79.2% of the specific discharge capacity retention under the same conditions.

Zhang *et al.*[68] employed a similar PANI intercalation strategy, albeit in a metal–organic framework (MOF)-derived V_2O_5. The high specific surface area, complemented by the intercalated

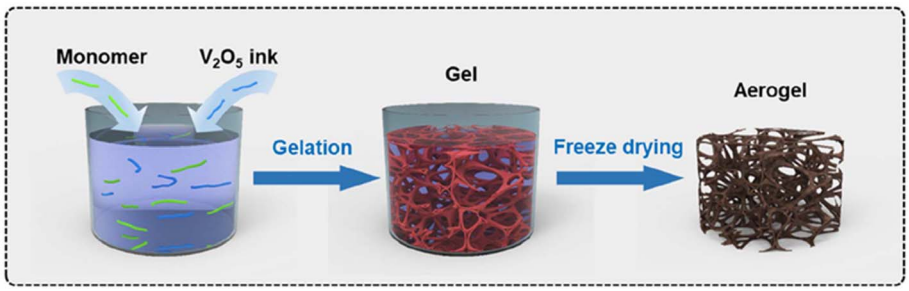

Fig. 9 Schematic diagram of the preparation of 2D PEDOT/V_2O_5 in the aerogel state. Reprinted from ref. 64, copyright (2022), with permission from RSC.

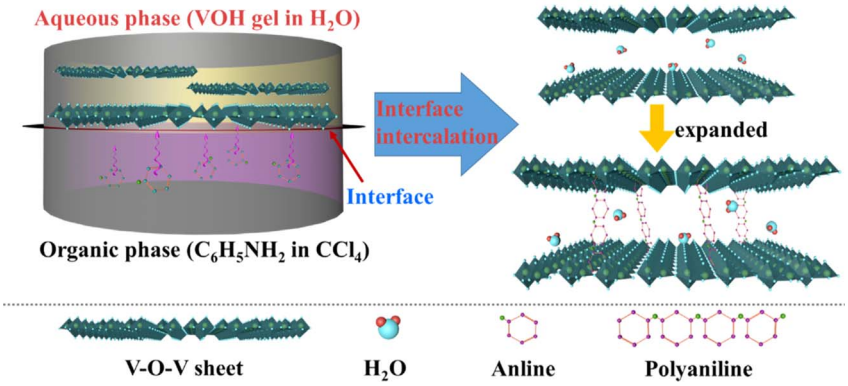

Fig. 10 Schematic illustration of the prepared route of the PANI–VOH by the interface-intercalation method. Reprinted from ref. 61, copyright (2021), with permission from Elsevier.

PANI, provided abundant accessible electrochemical active sites and shortened the ions transfer pathways. The outcome was a composite material that exhibited a high discharge capacity of 450 mAh g^{-1} at 0.5 A g^{-1}, a notable increase compared to the 210 mAh g^{-1} in the case of bare V_2O_5.

Collectively, these studies provide compelling evidence that the intercalation or coating of vanadium-based cathodes with conductive polymers holds a promising potential for enhancing the performance of A-ZIBs. Increasing the interlayer spacing, enhancing the electrical conductivity, and maintaining the structural stability for prolonged times, the use of polymers with vanadium oxide-based materials leads to enhanced Zn^{2+} diffusion, improved structural stability, and higher discharge capacity. Therefore, the application of conductive polymers demonstrates its critical role in the development of high-performance vanadium-based cathodes.

3.2 A-ZIBs based on manganese oxides

Recent research aims to alleviate the typical limitations associated with manganese-based cathode materials for A-ZIBs, such as the low electronic conductivity and the excessive dissolution of manganese, by incorporating conductive polymers in the manganese oxide lattice. The resulting electrochemical performances are very broad, most probably due to the various methods used to synthesize the manganese oxides, to polymerize the polymers, and to prepare and test the electrodes (*i.e.* in terms of current rates, active material mass loading, *etc.*). However, a commonality observed with all the strategies is the reduced manganese dissolution as depicted in Fig. 13a. Research by Huang *et al.*[75] showed that a surface coating of PPy on MnO_2, can effectively alleviate the dissolution of manganese. Notably, their DFT and X-ray photoelectron spectroscopy data suggested that a bond between manganese and nitrogen (Mn–N) was readily created at the interface of MnO_2 and PPy (Fig. 13b). This bond formation led to a decrease in the surface threshold energy and the energy required for Zn^{2+} adsorption. Their PPy-coated MnO_2 showed significantly improved cyclic stability at both low and high current densities, with negligible capacity fading at 1 A g^{-1} for 500 cycles.

The incorporation of conductive polymers into manganese oxide can be carried out through different synthesis routes, such as hydrothermal oxidation reactions or simple surface

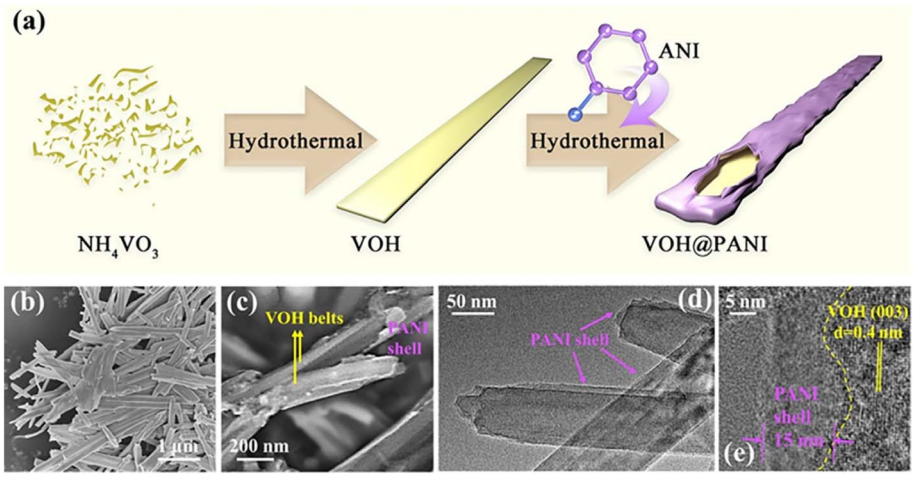

Fig. 11 (a) Schematic synthetic route, (b and c) FE-SEM images, (d and e) TEM and HRTEM images of VOH@PANI core–shell structures. Reprinted from ref. 69, copyright (2023), with permission from Elsevier.

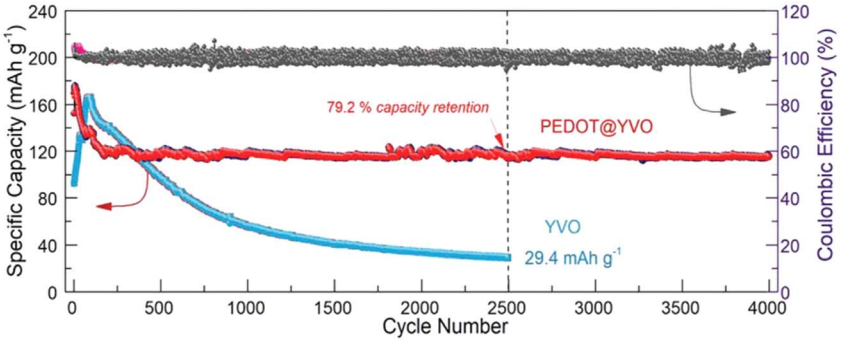

Fig. 12 High-rate stable performance of cells with mass loading of 1.8 mg of YVO and PEDOT@YVO at 1C. Reprinted from ref. 71, copyright (2021), with permission from Wiley.

coatings. Various polymerization temperatures, ranging between 0 to 120 °C, and oxidizing agents such as ferric chloride and ammonium persulfate have been employed in recent research.

Ruan *et al.*[76] addressed the issue of the manganese dissolution from MnO_2 in an A-ZIB by depositing MnO_2 onto carbon cloth through a hydrothermal reaction followed by a self-initiated polymerization of PANI on the manganese oxide's surface. This resulted in an increase of 20% of the specific discharge capacity (286 mAh g^{-1} at 0.5 A g^{-1}). Additionally, an increase of the cycle life of the electrode at a very high current rate of 4.0 A g^{-1} was observed.

Liao *et al.*[77] fabricated a β-MnO_2–PPy composite *via* a hydrothermal treatment of $MnSO_4$, APS, and PPy nanowires in an aqueous mixture at 120 °C. The resulting material delivered a specific discharge capacity of 175 mAh g^{-1} at a current density

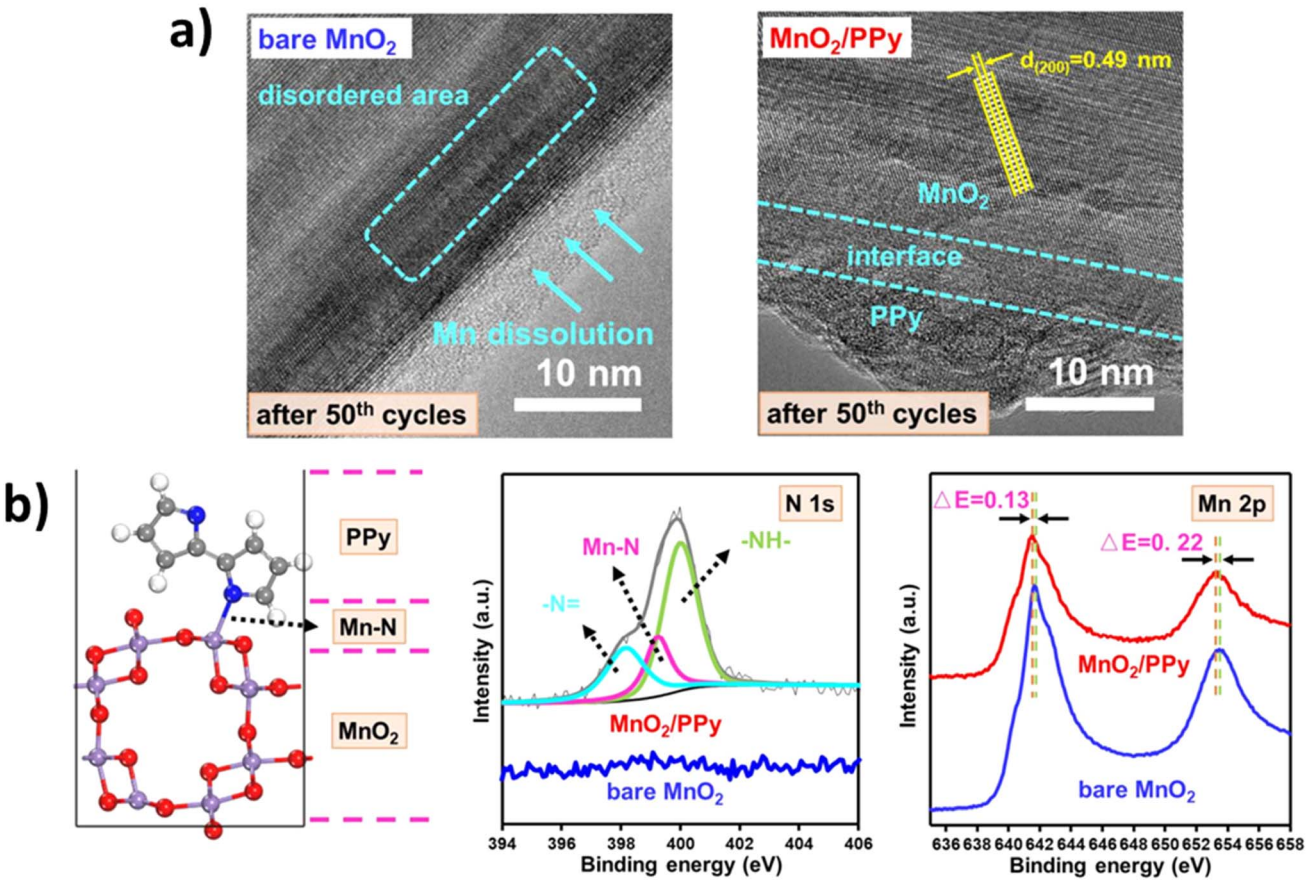

Fig. 13 (a) *Ex situ* HRTEM image after 50 cycles of bare MnO_2 and MnO_2/PPy. (b) Optimal configuration of the disordered MnO_2 surface covered by the PPy; N 1s high resolution XPS spectra and Mn 2p high resolution XPS spectra of MnO_2/PPy and bare MnO_2. Reprinted from ref. 75, copyright (2020), with permission from Elsevier.

of 0.5 A g^{-1}, a significant increase from the 50 mAh g^{-1} of the bare β-MnO_2. This enhancement was attributed to the high conductivity of the PPy nanowires and the resulting 3D mesoporous microsphere structure formed by the combination of the β-MnO_2 nanorods and the PPy nanowires.

Some researchers have explored eco-friendlier and less intense alternatives for synthesizing MnO_2-conductive polymer composites. In this regard, Chen *et al.*[78] and Wang *et al.*[79] proposed a synthesis in which PEDOT-intercalated MnO_2 was formed through a redox reaction between $KMnO_4$, $MnSO_4$, and EDOT monomers in an ice bath as depicted in Fig. 14. In a 2 M $ZnSO_4$ + 0.2 M $MnSO_4$ electrolyte, both studies reported an improved discharge capacity of *ca.* 220 mAh g^{-1} at 0.5 A g^{-1} and an enhanced cycling stability compared to bare MnO_2, probably due to an increased diffusion kinetics and a reinforced crystal structure.

Conductive polymer coatings strategies have also been followed in preparing manganese-based cathode materials. Kamenskii *et al.*[80] coated the surface of δ-MnO_2 particles with PEDOT:PSS by mechanically mixing them in an aqueous dispersion at room temperature. The resulting PEDOT:PSS-coated δ-MnO_2 delivered an initial specific discharge capacity of 280 mAh g^{-1} at a current density of 0.5 A g^{-1}, which is doubled compared to the one delivered by the bare δ-MnO_2. Their coated material retained 99% of its capacity after 100 cycles *versus* 89% in the case of bare δ-MnO_2 in 2 M $ZnSO_4$ + 0.1 M $MnSO_4$ at 0.3 A g^{-1}.

Due to the inferior electric conductivity of manganese-based cathodes in A-ZIBs, other substances like reduced graphene oxide (rGO) and carbon nanotubes (CNTs) might be incorporated along with conductive polymers. For example, Mao *et al.*[81] crafted a PANI-coated aerogel of MnO_2 and rGO by using rGO in combination with PANI, polymerized through APS as the polymerization agent. The manganese dissolution was considerably limited, and the material retained 82.7% of its initial specific capacity after 600 cycles at 0.1 A g^{-1} while showing an initial specific discharge capacity of 241.1 mAh g^{-1}. Niu *et al.*[82] implemented a similar method to boost the conductivity of α-MnO_2. The inclusion of PPy improved the cycling stability and their α-MnO_2/rGO–PPy provided a discharge capacity of about 240 mAh g^{-1} at 0.5 A g^{-1}, which is higher than the 160 mAh g^{-1} of the pure α-MnO_2.

Using CNTs, HCl, and pyrrole monomers mixed with MnO_2 nanowires in an ice bath, Zhang *et al.*[83] proposed a free-standing flexible film (CNT/MnO_2–PPy), which displayed a higher cycling stability in comparison to the bare CNT/MnO_2. The 220 mAh g^{-1} initial discharge capacity of the bare electrode reduced to only 70 mAh g^{-1} after 200 cycles at 0.3 A g^{-1}, while CNT/MnO_2–PPy showed no capacity fading under the same cycling conditions, resulting from enhanced conductivity of MnO_2 and prevention of manganese dissolution.

Iron doping is another technique to enhance the Zn^{2+} (de) insertion kinetics with manganese-based cathodes. Xu *et al.*[84] combined the benefits of enlarged α-MnO_2 lattice spacing by pre-intercalating Fe^{3+} during the formation of α-MnO_2 crystals with the benefits of PPy coatings. This method resulted in a facilitated (de-)intercalation of Zn^{2+}, a reduced volume variation during cycling, and a considerable 60% increase in the initial discharge capacity of their cathode material.

In conclusion, while each of these studies utilizes a unique approach, there is a consistent emphasis on the role of conductive polymers in overcoming the inherent limitations of manganese oxides. Improved conductivity and energy density, alleviated manganese dissolution, and improved cycling stability were obtained in recent literature regardless of the type of manganese oxide or the synthesis route.

3.3 A-ZIBs based on Prussian blue analogues

The relatively shorter cycle life of PBAs in A-ZIBs remains a challenge to overcome, particularly when compared to the commercial insertion materials used in organic LIBs. Nonetheless, higher operating potential compared to the manganese oxide and especially to the vanadium oxides and lower costs make the materials from the PBAs family very appealing for A-ZIBs. Moreover, the flexible nature of the coordination chemistry of PBAs allows for enhancements in their electrochemical performance and durability through modifications in their synthesis conditions, such as the duration and the temperature of the reaction, reactant concentrations, and thermal treatment.[85] These alterations influence aspects like the positioning of the elements, the potassium or iron content, and the quantity of coordinated water within the material lattice.[85,86] Despite the potential to improve PBAs' stability and electrochemical properties by varying their synthesis conditions, the determination of the optimal method continues to be challenging.

A practical strategy to augment the electrochemical performance and overcome the cycle life restrictions of PBAs involves applying conductive polymer coatings on their surfaces. Such coatings can serve as a protective shield that slows down the degradation or dissolution rate of PBAs.

To the best of our knowledge, there are only a few studies on the use of conductive polymer together with PBAs in A-ZIBs either as composites or coatings, despite their promising properties. In a recent study, Baghodrat *et al.*[87] investigated the use of PEDOT:PSS as a conductive polymer coating to enhance the performance of copper hexacyanoferrate (CuHCF) in A-ZIBs. After assessing the electrochemical stability of the PEDOT:PSS-coated CuHCF particles in the electrolyte and potential range used for the experiments, the synthesized CuHCF particles were coated with varying concentrations of PEDOT:PSS, identifying

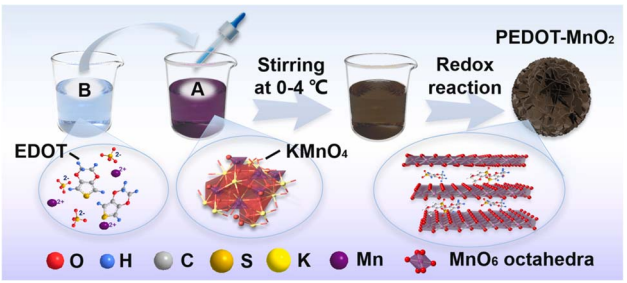

Fig. 14 Schematic diagram of the preparation process. Reprinted from ref. 78, copyright (2023), with permission from Elsevier.

an optimal coating dispersion concentration of 4.5 wt%. This concentration provided a balance between improved electrochemical performance and material efficiency. Moreover, morphological and compositional analysis confirmed that PEDOT:PSS forms a uniform coating on the CuHCF particles without altering their crystallinity, indicating that the polymer acts as a surface coating rather than intercalating into the CuHCF structure. The PEDOT:PSS-coated CuHCF exhibited significantly improved cycle life and maintained high coulombic efficiency during their galvanostatic cycling at a current rate of 1C with electrodes having an active material mass loading of *ca.* 10 mg cm^{-2}. Specifically, the optimal electrode retained 80% of the initial discharge energy after approximately 700 cycles at a current rate of 1C, compared to only 400 cycles for the uncoated electrode. The study demonstrated that the PEDOT:PSS coating effectively mitigated the degradation of CuHCF, delaying the onset of its phase transitions during cycling while maintaining high coulombic efficiency (≥99.5%) and without affecting the rate-capability of the material (Fig. 15).

Additionally, the benefits of using PPy to enhance the electrochemical performance of manganese hexacyanoferrate (MnHCF), a member of the PBA family, were reported in the work of Chen *et al.*[54] By mixing MnHCF particles in an ice bath with various amounts of pyrrole monomers and APS as the polymerization agent, PPy-coated cubic particles of MnHCF have been synthesized (Fig. 16). The resulting material showed a discharge capacity of *ca.* 107.6 mAh g^{-1} after 100 cycles at 0.1 A g^{-1}, while the bare MnHCF only retained *ca.* 55 mAh g^{-1} in the same experimental conditions. A similar approach was followed by Puthiyaveetil *et al.*,[88] coating Vanadium-based Prussian blue analogue (V-PBA) with PPy. The synthesis involved first generating V-PBA *via* a precipitation reaction between vanadium and ferricyanide ions, followed by an *in situ* oxidative polymerization of pyrrole. Electrochemical evaluations demonstrated that the optimally coated composite (V-PBA/PPy) exhibited a higher specific capacity (173 mAh g^{-1} at 0.10 A g^{-1}) compared to the uncoated V-PBA (80 mAh g^{-1}). Furthermore, the V-PBA/PPy electrode maintained 85% of its initial capacity over 500 cycles while the uncoated electrode degraded to 68%.

Liu *et al.*[89] applied PANI onto the zinc hexacyanoferrate (ZnHCF) surface under certain pH and temperature conditions, leading to a 50% increased initial specific discharge capacity. The PANI coating hindered the ZnHCF dissolution, and, as a result, the material retained 65% of its initial specific discharge capacity after 300 cycles at 0.5 A g^{-1}. On the contrary, the specific capacity of the uncoated ZnHCF decreased to 49% under the same cycling conditions. The PANI-coated ZnHCF also exhibited a high stretchability of 600% while maintaining stable electrochemical properties, adding another dimension to the versatility and applicability of polymer coatings.

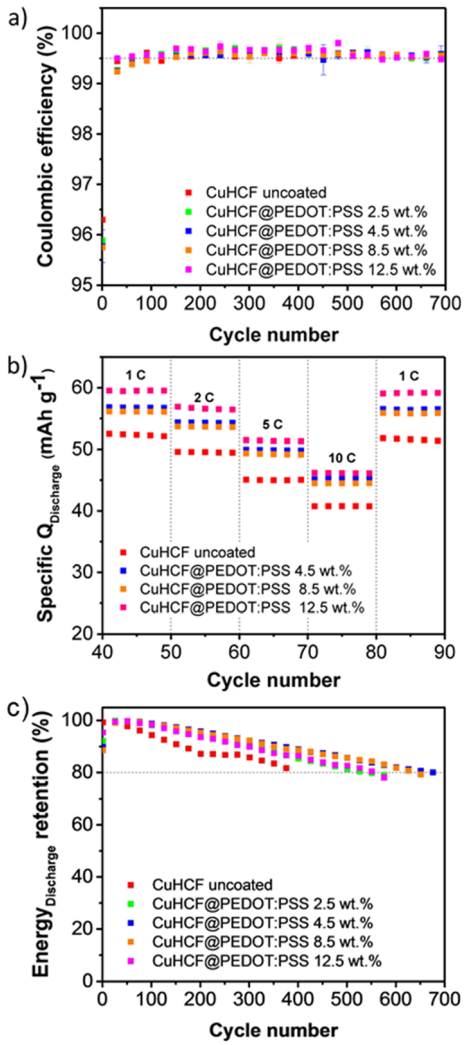

Fig. 15 (a) Average value of coulombic efficiency of the synthesized CuHCF-based electrodes, coated with various amounts of PEDOT:PSS and galvanostatically cycled at 1C. Mean values and standard deviations have been obtained averaging at least three measurements. (b) Galvanostatic power test of uncoated CuHCF and coated CuHCF@-PEDOT:PSS electrodes with different amount of PEDOT:PSS in the coating. (c) Average discharge energy retention of the synthesized CuHCF-based electrodes uncoated and coated with different amounts of PEDOT:PSS galvanostatically cycled at 1C. Mean values and standard deviations have been obtained, averaging at least three measurements. Reprinted from ref. 87, copyright (2024), with permission from the authors.

4. Calling for standardization

As seen in the previous sections, the use of conductive polymers as coatings/additives for the active material or within the formulation of the electrode is a promising strategy to enhance the electrochemical performance of the cathode materials for aqueous Zn-ion batteries. On the other hand, several critical aspects in the research works need to be addressed to achieve a more accurate, relevant, and practical knowledge of these systems.

A troubling trend in the current literature is using unrealistic charge–discharge rates (*i.e.* current rates or C-rates), which prohibits any effective comparison between the different research works and undermines the validity of many studies, particularly when assessing key performance indicators such as the cycle life or the nominal capacity. While it may be tempting

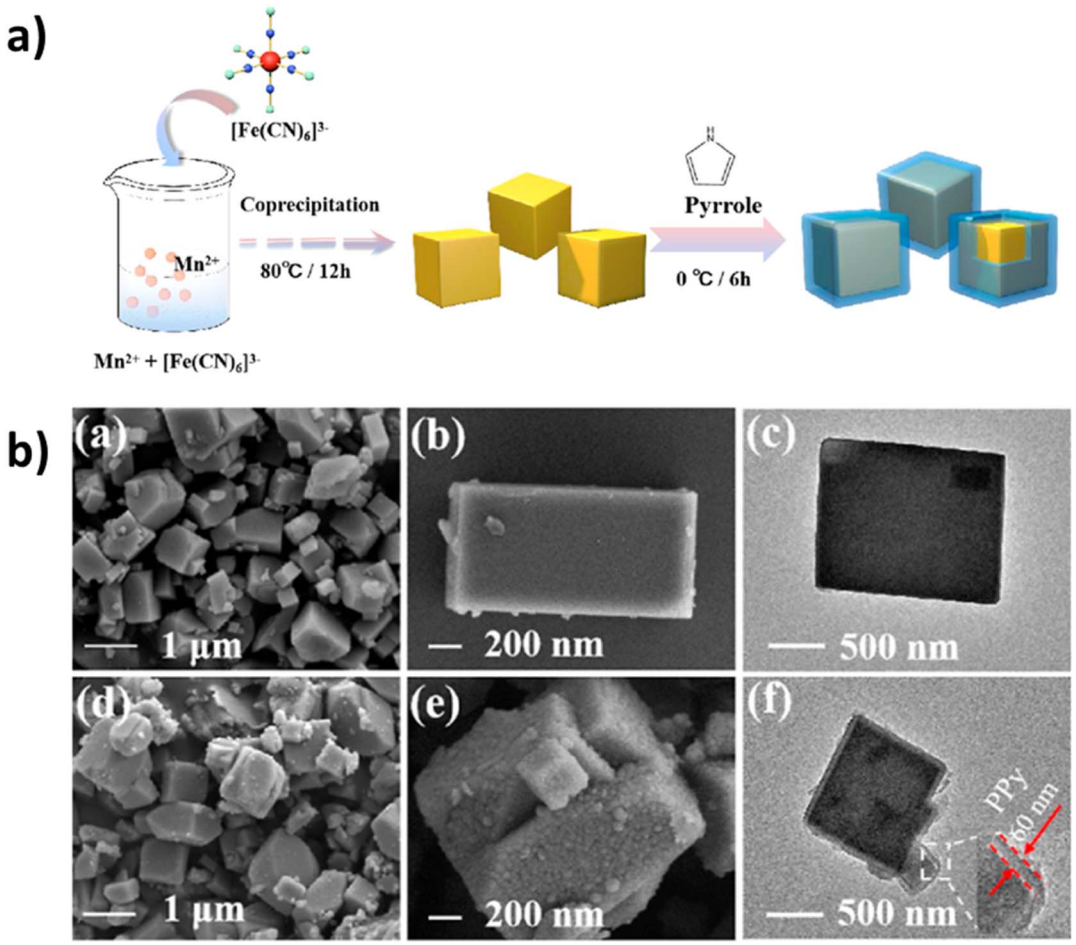

Fig. 16 (a) Schematic illustration of KMHCF and KMHCF@PPy sample. (b(a and b)) SEM and (c) TEM images of KMHCF. (d and e) SEM and (f) TEM images of KMHCF-30. Reprinted from ref. 54, copyright (2022), with permission from ACS.

to use very high currents to yield impressive cycle life, such parameters often do not hold and are not transferable to the real conditions of A-ZIBs during their operation as stationary energy storage systems.[6] In fact, grid-scale energy storage systems operate under vastly different conditions, however ranging usually between 0.5C–2C, without exceeding 10C (meaning full discharge/charge of the system in 6 minutes). In particular, it has been shown that grid-scale energy storage systems operate around 0.5C–1C for more than 97% of the time with an average peak of 3.5C during their cycle duty.[90]

Therefore, the cycle life of A-ZIBs materials should be assessed at the typical current rates utilized for the energy grid,[6,91] since thousands of cycles obtained at a current density ≥ 1 A g^{-1} do not directly prove that the same cycle life can be obtained at a more application-relevant current density of *ca.* 0.1 A g^{-1}. Unfortunately, an alarmingly high number of studies disregard this crucial factor, and the cycle life of A-ZIBs materials is usually assessed at very high current rates.

Similarly, numerous studies fail to report the mass loadings of the active materials present within the electrodes used for the reported experiments. This is an alarmingly critical omission, as the mass loading of the active material present within the electrode formulation significantly affects the battery performance and is needed to convert operational currents into C-rates and *vice versa*. Moreover, most of the published literature, when not omitting it, reports very low mass loadings of the active material used for the electrode preparation (*ca.* 1–2 mg cm^{-2}), far below the industrial standard, showing performances under mass loading conditions that are not relevant for the application. As highlighted by Lin *et al.*,[92] such low mass loadings artificially improve the electrochemical performance by drastically reducing the diffusion limitations and increasing the electrical contact between the particles, resulting in negligible polarization effects. An operation-relevant evaluation of batteries in general and aqueous Zn-ion batteries in particular would require the use of electrodes with active materials mass loadings of at least *ca.* 7–10 mg cm^{-2}.[6,92,101]

To further stress the problems in the literature discussed so far, the results reported in the published literature on the effect of the polymeric coating/composites on the performance of the cathode materials for aqueous Zn-ion batteries are summarized in Table 2. Relevant parameters have been included to ensure a meaningful and fair comparison of the published results, such as: mass loading of the active materials (when reported),

specific capacity at the current employed for the assessment of the cycle life, areal capacity, specific current used for assessing the cycle life, actual C-rate obtained at the current employed for the cycle life assessment (which in most cases is different than the nominal C-rate calculated based on the theoretical specific capacity of the material), cycle reached at the reported capacity retention, normalized cycle life with respect to the actual C-rate of the experiment assessing the cycle life.

The normalized cycle life has been chosen to attempt a comparison of the performance reported in the literature but obtained using a great variety of experimental conditions, thus providing a rough comparison across studies performed at different rates. However, it is not an absolute predictor of the durability of the systems, *i.e.*, cycling at low current density for a limited number of cycles cannot be directly equated to high-rate, long-term stability. At the same time, a long cycle life obtained at very high C-rates does directly imply an equally long-term cycling stability when operating conditions close to the ones required by the power-grid are used. We encourage future studies on aqueous Zn-ion batteries in general to report cycle

Table 2 Comparison of the works reported in the literature using of polymeric coatings/composites on the performance of different active materials for aqueous Zn-ion batteries. The published results have been ordered from higher to lower areal capacity

Polymer	Active material	Additives	Electrolyte	Mass loading (mg cm^{-2})	Initial specific capacity (mAh g^{-1})	Areal capacity (mAh cm^{-2})	Actual C-rate	Specific current (A g^{-1})	Cycle life at reported capacity retention (%)	Normalized cycle life C-life/C-rate	Ref.
PANI	V_2O_5	—	3 M $Zn(OTF)_2$	5.00	325	1.62	3.07	1.0	600 at 80%	228	74
PEDOT:PSS	V_2O_5	—	3 M $Zn(CF_3SO_3)_2$	3.50	260	0.91	19.2	5.0	2000 at 89.4%	104	65
PEDOT	V_2O_5	—	3 M $ZnSO_4$	2.00	350	0.70	2.8	1.0	100 at 97.1%	35	66
PEDOT	V_2O_5	—	3 M $Zn(CF_3SO_3)_2$	2.00	325	0.65	30.8	10.0	3000 at 80%	97	93
PANI	V_2O_5	—	3 M $Zn(CF_3SO_3)_2$	2.00	325	0.65	24.6	8.0	2000 at 91.8%	81	68
PEDOT:PSS	CuHCF	—	0.1 M $ZnSO_4$	10.00	57	0.57	1.7	0.1	700 at 80%	411	87
PEDOT	V_2O_5	—	2 M $Zn(CF_3SO_3)_2$	2.00	293	0.59	0.34	0.1	100 at 88.7%	294	94
PANI	V_2O_5	—	3 M $Zn(CF_3SO_3)_2$	1.75	275	0.48	18.2	5.0	250 at 80%	14	61
PEDOT	V_2O_5	—	2 M $Zn(OTF)_2$	1.50	300	0.45	0.6	0.2	40 at 80%	167	95
PEDOT	MnO_2	—	2 M $ZnSO_4$ + 0.2 M $MnSO_4$	3.50	125	0.44	16.0	2.0	1500 at 120%	93	78
PANI	V_2O_5	—	3 M $Zn(CF_3SO_3)_2$	2.00	220	0.44	9.0	2.0	2000 at 102%	222	69
PEDOT	V_2O_5	CNT	3 M $ZnSO_4$	2.00	190	0.38	52.6	10.0	1000 at 94.7%	19	64
PPy	V_2O_5	—	3 M $Zn(CF_3SO_3)_2$	1.20	300	0.36	16.6	5.0	2000 at 97%	120	63
PPy	MnO_2	Iron doped	2 M $ZnSO_4$ + 0.1 M $MnSO_4$	1.00	335	0.33	0.3	0.1	40 at 80%	133	84
PANI	V_2O_5	—	3 M $Zn(CF_3SO_3)_2$	1.95	170	0.33	23.5	4.0	800 at 80%	34	96
PPy	MnO_2	—	2 M $ZnSO_4$ + 0.1 M $MnSO_4$	1.15	91	0.10	10.9	1.0	500 at 114%	45	75
PPy	MnO_2	rGO	3 M $Zn(CF_3SO_3)_2$	1.20	240	0.29	2.0	0.5	100 at 87.5%	50	82
PPy	V_2O_5	—	2 M $ZnSO_4$	1.75	110	0.19	9.1	1.0	300 at 91%	33	70
PEDOT	MnO_2	CNT	2 M $ZnSO_4$ + 0.2 M $MnSO_4$	1.00	135	0.13	14.8	2.0	1000 at 89%	75	79
PANI	MnO_2	rGO	2 M $ZnSO_4$	1.10	120	0.13	8.3	1.0	600 at 91.6%	72	81
PPy	V-PBA	—	1 M $Zn(CF_3SO_3)_2$	1.00	120	0.12	8.3	1.0	500 at 85%	60	88
PANI	V_2O_5	—	2 M $ZnSO_4$	1.10	100	0.11	5.0	0.5	500 at 117%	100	97
PPy	MnHCF	—	2 M $ZnSO_4$ + 0.1 M $MnSO_4$	1.50	60	0.09	8.3	0.5	500 at 108%	60	54
PANI	ZnHCF	—	$ZnCl_2$	1.00	75	0.07	6.6	0.5	90 at 80%	13	89
PEDOT	V_2O_5	—	3 M $Zn(CF_3SO_3)_2$	**Not reported**	375	**Unknown**	1.3	0.5	100 at 80%	77	72
PEDOT:PSS	MnO_2	—	2 M $ZnSO_4$ + 0.1 M $MnSO_4$	**Not reported**	260	**Unknown**	1.2	0.3	110 at 99%	100	80
PPy	V_2O_5	—	3 M $Zn(CF_3SO_3)_2$	**Not reported**	283	**Unknown**	14.1	4.0	1350 at 80%	95	73
PPy	V_2O_5	—	3 M $Zn(CF_3SO_3)_2$	**Not reported**	306	**Unknown**	32.7	10.0	760 at 80%	23	62
PPy	V_2O_5	—	3 M $Zn(CF_3SO_3)_2$	**Not reported**	225	**Unknown**	44.4	10.0	2000 at 100%	45	67
PPy	MnO_2	CNT	2 M $ZnSO_4$ + 0.1 M $MnSO_4$	**Not reported**	250	**Unknown**	4.0	1.0	1000 at 96.7%	250	83
PPy	MnO_2	—	2 M $ZnSO_4$ + 0.1 M $MnSO_4$	**Not reported**	350	**Unknown**	0.6	0.2	160 at 97%	266	77
PPy	NMHCF	—	1 M $Zn(CF_3SO_3)_2$ + 1 M $NaCF_3SO_3$	**Not reported**	55	**Unknown**	3.6	0.2	150 at 86.5%	42	98
PANI	V_2O_5	K^+	3 M $Zn(CF_3SO_3)_2$	**Not reported**	337	**Unknown**	14.8	5.0	3000 at 89.6%	181	99
PANI	V_2O_5	Ni^{2+}	3 M $Zn(CF_3SO_3)_2$	**Not reported**	261	**Unknown**	19.1	5.0	1000 at 89.5%	52	100
PANI	MnO_2	—	2 M $ZnSO_4$ + 0.1 M $MnSO_4$	**Not reported**	177	**Unknown**	22.8	4.0	9000 at 96.9%	394	76

life data until a common capacity retention threshold (*e.g.*, 80%) is reached at a given C-rate, and to use realistic C-rates in the experiments. This would result in a fairer and more accurate comparison of cycle life performance across different research works.

This clear lack of standardization and the discrepancy between laboratory tests and realistic operational conditions, dictated by the grid-scale storage sector, greatly undermines the comparability of the different studies, reduces the overall value and reputation of the research landscape, and delays the development and distribution of the A-ZIB technology.

Another critical issue is that in the majority of cases the electrochemical stability of the conductive polymers is ignored even if it depends greatly on the electrolytes and on the operating potentials used in combination with the specific active materials. Many researchers use conductive polymers in A-ZIBs without first verifying the voltage stability window of the polymer in their systems. As an example, it is well known that PEDOT is subject to degradation and over-oxidation at high potentials of about 1.7 V *vs.* Zn^{2+}/Zn, particularly in acidic environments.[33–36] However, most studies fail to consider these findings when employing PEDOT in A-ZIBs, even if the electrolyte is typically mildly acidic. The electrochemical stability of conductive polymers (not only restricted to the use or PEDOT) within the voltage window of the battery system is a critical element in the cell's lifespan and coulombic efficiency. Overlooking these aspects may lead to misleading results and may undermine the validity of the research work.

Similarly, many studies often overlook the thermal stability of conductive polymers. For instance, it has been shown in the literature that the electrical conductivity of various conductive polymers, *e.g.*, PEDOT:PSS, increases with increasing temperature up to >150 °C.[38] However, cathode materials are more prone to degradation at high temperatures. As an example, it has been demonstrated that the electrochemical performance of PBAs is susceptible to thermal annealing, leading to detrimental structural rearrangements at temperatures exceeding 125 °C.[85] Thus, in this case, the thermal stability and the electrical conductivity of the resulting electrode based on a material belonging to the PBA family and PEDOT:PSS are restricted to the thermal stability window of the PBA used as active material.

Because some conductive polymers such as PPy and PEDOT have very low Zn^{2+} storage capacities, exceeding a certain polymer concentration leads to inactivity toward the electrochemical Zn^{2+} (de-)insertion reactions and, therefore, to lower specific capacities. Accordingly, researchers are encouraged to investigate the effect of different polymer concentrations, to optimize its amount and look for an optimal wt% range to find a balance between ion storage capacity, cycle life, and conductivity.

To ensure clarity and precision in reporting the experimental results, it is crucial to specify the composition of the cathode material, including the specific proportions of the active material and conductive polymer. Thermogravimetric analysis (TGA) can offer valuable insights into the material's composition, provided that the material's stability permits this analysis. For polymer coatings, the composition of the coating solution must be specified. Moreover, researchers should preferably calculate the specific discharge capacity and the C-rate based solely on the weight of the active material, excluding the weight of the polymer. Last but not the least, any influence of the presence of the polymer within the electrode when observed on the specific discharge capacity should be highlighted and discussed.

Additionally, when research studies employ non-commercial conductive polymers, it becomes crucial to report their essential characteristics. Key information, such as the degree of doping and the electrical conductivity, which have substantial effects on the electrochemical performance and the mechanical properties of the cathode, is unfortunately often missing in the literature. This lack of transparency further hampers the comparability of different studies and their collective contribution to the field of aqueous-based post-Li-ion systems in general and of aqueous Zn-ion batteries in particular.

In light of all of these observations, there is an immediate need for a comprehensive standardization in the research methodology and in the experimental information reported in the studies regarding the aqueous Zn-ion technology. Adopting relevant operational parameters in the design of the experimental study, ensuring a complete disclosure of all the relevant experimental conditions, and paying careful attention to the system-specific stability issues should be integral parts of the future research on A-ZIBs.

Fostering these good research practices can concretely pave the way for more meaningful comparisons between different research studies, enhance the reproducibility, and ultimately expedite the progress of aqueous Zn-ion batteries toward real-life applications.

5. Conclusion

This review assessed the recent efforts directed at improving the electrochemical performance of the three primary families of cathode materials for aqueous zinc-ion batteries, namely vanadium oxides, manganese oxides, and Prussian blue analogues *via* the integration of conductive polymers such as PEDOT, PEDOT:PSS, PPy, and PANI. The resulting cathode materials have shown boosted discharge capacity, extended cycle life, and elevated electrical conductivity.

Our review highlighted that conductive polymers, when embedded within the V_2O_5 structure, not only enlarge the interlayer spacing, promoting a faster Zn^{2+} (de-)insertion, but also enhance material stability and, thus, the cycle life of V_2O_5. Manganese oxides, which intrinsically suffer from low conductivity and manganese dissolution during repeated charge and discharge cycles, have shown significantly improved stability and reduced dissolution rates when combined with conductive polymers. Lastly, while PBAs suffer from a short cycle life, their cost-effectiveness and high operating potential have made them attractive candidates for A-ZIBs. The conductive polymer coatings applied to these materials seem to effectively slow their degradation rate and enhance their overall performance.

However, these encouraging advancements are accompanied by severe challenges rooted in the current research practices.

The transition from controlled laboratory conditions to realistic applications is fraught with complexities. Issues such as the use of unrealistic testing parameters, gaps in data reporting, and overlooking the critical characteristics of conductive polymers can distort the understanding of the true potential of the use of conductive polymers in combination with the cathode materials and can impact the subsequent research trajectory.

By aligning research practices with real-world scenarios and ensuring complete transparency in reporting, findings remain relevant and actionable. This transition is not just a matter of scientific integrity but of practical urgency, given the escalating global demand for reliable, green and cost-effective energy storage solutions.

Looking ahead, several research directions hold significant promise for advancing the role of conductive polymers in A-ZIBs. Developing next-generation polymers, through innovative chemical design, functionalization and doping strategies, could broaden their electrochemical stability windows while maintaining high conductivity and high mechanical stability. Hybrid systems that integrate conductive polymers with carbon nanostructures may further enhance these characteristics. In parallel, the use of *in situ* and *in operando* characterization techniques, including XRD, IR spectroscopy, and electron microscopy, will be crucial for elucidating the polymer–cathode interactions and for identifying the mechanisms underlying their degradation. Equally important is the adaptation of polymer processing to sustainable and scalable electrode fabrication methods to bridge the gap between the research at the laboratory scale and their actual industrial application. Together, these efforts will be central to unlocking the full potential of conductive polymers as key enablers of high-performance, durable, and economically viable A-ZIBs.

Conflicts of interest

The authors declare no conflict of interest.

Data availability

No primary research results, software or code have been included and no new data were generated or analysed as part of the review.

Acknowledgements

The financial support of the Federal Ministry of Research, Technology and Space (BMFTR) in the frame of the project "ZIB2" (FKZ 03XP0523B) is gratefully acknowledged.

References

1 Y. Liu, X. Lu, F. Lai, T. Liu, P. R. Shearing, I. P. Parkin, G. He and D. J. L. Brett, Rechargeable Aqueous Zn-Based Energy Storage Devices, *Joule*, 2021, **5**, 2845–2903.
2 X. Jia, C. Liu, Z. G. Neale, J. Yang and G. Cao, Active Materials for Aqueous Zinc Ion Batteries: Synthesis, Crystal Structure, Morphology, and Electrochemistry, *Chem. Rev.*, 2020, **120**, 7795–7866.
3 X. Min, J. Xiao, M. Fang, W. Wang, Y. Zhao, Y. Liu, A. M. Abdelkader, K. Xi, R. V. Kumar and Z. Huang, Potassium-Ion Batteries: Outlook on Present and Future Technologies, *Energy Environ. Sci.*, 2021, **14**, 2186–2243.
4 M. Görlin, D. O. Ojwang, M. T. Lee, V. Renman, C. W. Tai and M. Valvo, Aging and Charge Compensation Effects of the Rechargeable Aqueous Zinc/Copper Hexacyanoferrate Battery Elucidated Using in Situ X-Ray Techniques, *ACS Appl. Mater. Interfaces*, 2021, **13**, 59962–59974, DOI: 10.1021/acsami.1c19167.
5 J. Ming, J. Guo, C. Xia, W. Wang and H. N. Alshareef, Zinc-Ion Batteries: Materials, Mechanisms, and Applications, *Mater. Sci. Eng., R*, 2019, **135**, 58–84, DOI: 10.1016/J.MSER.2018.10.002.
6 G. Zampardi and F. La Mantia, Open Challenges and Good Experimental Practices in the Research Field of Aqueous Zn-Ion Batteries, *Nat. Commun.*, 2022, **13**, 1–5, DOI: 10.1038/s41467-022-28381-x.
7 M. Tribbia, G. Zampardi and F. La Mantia, Towards the Commercialization of Rechargeable Aqueous Zinc Ion Batteries: The Challenge of the Zinc Electrodeposition at the Anode, *Curr. Opin. Electrochem.*, 2023, 101230.
8 M. Xu, J. Chen, Y. Zhang, B. Raza, C. Lai and J. Wang, Electrolyte Design Strategies towards Long-Term Zn Metal Anode for Rechargeable Batteries, *J. Energy Chem.*, 2022, **73**, 575–587.
9 W. Lu, C. Zhang, H. Zhang and X. Li, Anode for Zinc-Based Batteries: Challenges, Strategies, and Prospects, *ACS Energy Lett.*, 2021, **6**, 2765–2785.
10 X. Wang, Z. Zhang, B. Xi, W. Chen, Y. Jia, J. Feng and S. Xiong, Advances and Perspectives of Cathode Storage Chemistry in Aqueous Zinc-Ion Batteries, *ACS Nano*, 2021, **15**, 9244–9272.
11 S. Zuo, X. Xu, S. Ji, Z. Wang, Z. Liu and J. Liu, Cathodes for Aqueous Zn-Ion Batteries: Materials, Mechanisms, and Kinetics, *Chem.–Eur. J.*, 2021, **27**, 830–860.
12 T. Zhou, L. Zhu, L. Xie, Q. Han, X. Yang, L. Chen, G. Wang and X. Cao, Cathode Materials for Aqueous Zinc-Ion Batteries: A Mini Review, *J. Colloid Interface Sci.*, 2022, **605**, 828–850, DOI: 10.1016/j.jcis.2021.07.138.
13 G. He, Y. Liu, D. E. Gray and J. Othon, Conductive Polymer Composites Cathodes for Rechargeable Aqueous Zn-Ion Batteries: A Mini-Review, *Compos. Commun.*, 2021, **27**, 100882, DOI: 10.1016/j.coco.2021.100882.
14 Y. Xu, G. Zhang, J. Liu, J. Zhang, X. Wang, X. Pu, J. Wang, C. Yan, Y. Cao, H. Yang, *et al.*, Recent Advances on Challenges and Strategies of Manganese Dioxide Cathodes for Aqueous Zinc-Ion Batteries, *Energy Environ. Mater.*, 2023, **6**, e12575, DOI: 10.1002/eem2.12575.
15 W. Shi, W. S. V. Lee and J. Xue, Recent Development of Mn-based Oxides as Zinc-Ion Battery Cathode, *ChemSusChem*, 2021, **14**, 1634–1658, DOI: 10.1002/cssc.202002493.
16 Y. Guo, Y. Zhang and H. Lu, Manganese-based Materials as Cathode for Rechargeable Aqueous Zinc-ion Batteries, *Battery Energy*, 2022, **1**, DOI: 10.1002/bte2.20210014.

17 P. Ruan, X. Xu, J. Feng, L. Yu, X. Gao, W. Shi, F. Wu, W. Liu, X. Zang, F. Ma, *et al.*, Boosting Zinc Storage Performance via Conductive Materials, *Mater. Res. Bull.*, 2021, **133**, 111077, DOI: 10.1016/j.materresbull.2020.111077.

18 T. Zhou, Q. Han, L. Xie, X. Yang, L. Zhu and X. Cao, Recent Developments and Challenges of Vanadium Oxides (VxOy) Cathodes for Aqueous Zinc-Ion Batteries, *Chem. Rec.*, 2022, **22**, e202100275, DOI: 10.1002/tcr.202100275.

19 E. G. Tolstopyatova, M. A. Kamenskii and V. V. Kondratiev, Vanadium Oxide–Conducting Polymers Composite Cathodes for Aqueous Zinc-Ion Batteries: Interfacial Design and Enhancement of Electrochemical Performance, *Energies*, 2022, **15**, 8966, DOI: 10.3390/en15238966.

20 G. Zampardi and F. La Mantia, Prussian Blue Analogues as Aqueous Zn-Ion Batteries Electrodes: Current Challenges and Future Perspectives, *Curr. Opin. Electrochem.*, 2020, **21**, 84–92, DOI: 10.1016/J.COELEC.2020.01.014.

21 G. Kasiri, J. Glenneberg, R. Kun, G. Zampardi and F. La Mantia, Microstructural Changes of Prussian Blue Derivatives during Cycling in Zinc-Containing Electrolytes, *ChemElectroChem*, 2020, **7**, 3301–3310, DOI: 10.1002/celc.202000886.

22 Y. Li, J. Zhao, Q. Hu, T. Hao, H. Cao, X. Huang, Y. Liu, Y. Zhang, D. Lin, Y. Tang, *et al.*, Prussian Blue Analogs Cathodes for Aqueous Zinc Ion Batteries, *Mater. Today Energy*, 2022, **29**, 101095, DOI: 10.1016/j.mtener.2022.101095.

23 B. Niu, J. Wang, Y. Guo, Z. Li, C. Yuan, A. Ju and X. Wang, Polymers for Aqueous Zinc-Ion Batteries: From Fundamental to Applications Across Core Components, *Adv. Energy Mater.*, 2024, **14**, 2303967, DOI: 10.1002/AENM.202303967.

24 L. Hu, J. Song, X. Yin, Z. Su and Z. Li, Research Progress on Polymer Solar Cells Based on PEDOT: PSS Electrodes, *Polymers*, 2020, **12**, 145, DOI: 10.3390/POLYM12010145.

25 S. Umoren and M. M. Solomon, Protective Polymeric Films for Industrial Substrates: A Critical Review on Past and Recent Applications with Conducting Polymers and Polymer Composites/Nanocomposites, *Prog. Mater. Sci.*, 2019, **104**, 380–450.

26 Y. Hui, C. Bian, J. Wang, J. Tong and S. Xia, Comparison of Two Types of Overoxidized PEDOT Films and Their Application in Sensor Fabrication, *Sensors*, 2017, **17**, 628, DOI: 10.3390/s17030628.

27 Z. Ma, W. Shi, K. Yan, L. Pan and G. Yu, Doping Engineering of Conductive Polymer Hydrogels and Their Application in Advanced Sensor Technologies, *Chem. Sci.*, 2019, **10**, 6232–6244, DOI: 10.1039/c9sc02033k.

28 Y. Wang, A. Liu, Y. Han and T. Li, Sensors Based on Conductive Polymers and Their Composites: A Review, *Polym. Int.*, 2020, **69**, 7–17, DOI: 10.1002/pi.5907.

29 P. P. Deshpande, N. G. Jadhav, V. J. Gelling and D. Sazou, Conducting Polymers for Corrosion Protection: A Review, *J. Coat. Technol. Res.*, 2014, **11**, 473–494, DOI: 10.1007/s11998-014-9586-7.

30 S. Tang, W. Guo and Y. Fu, Advances in Composite Polymer Electrolytes for Lithium Batteries and Beyond, *Adv. Energy Mater.*, 2021, **11**, 2000802, DOI: 10.1002/AENM.202000802.

31 P. Sengodu and A. D. Deshmukh, Conducting Polymers and Their Inorganic Composites for Advanced Li-Ion Batteries: A Review, *RSC Adv.*, 2015, **5**, 42109–42130, DOI: 10.1039/C4RA17254J.

32 I. Petsagkourakis, N. Kim, K. Tybrandt, I. Zozoulenko and X. Crispin, Poly(3,4-Ethylenedioxythiophene): Chemical Synthesis, Transport Properties, and Thermoelectric Devices, *Adv. Electron. Mater.*, 2019, **5**, 1800918, DOI: 10.1002/aelm.201800918.

33 J. F. Drillet, R. Dittmeyer, K. Jüttner, L. Li and K. M. Mangold, New Composite DMFC Anode with PEDOTas a Mixed Conductor and Catalyst Support, *Fuel Cells*, 2006, **6**, 432–438.

34 J. F. Drillet, R. Dittmeyer and K. Jüttner, Activity and Long-Term Stability of PEDOT as Pt Catalyst Support for the DMFC Anode, *J. Appl. Electrochem.*, 2007, **37**, 1219–1226, DOI: 10.1007/s10800-007-9393-2.

35 G. G. Láng, M. Ujvári, S. Vesztergom, V. Kondratiev, J. Gubicza and K. J. Szekeres, The Electrochemical Degradation of Poly(3,4-Ethylenedioxythiophene) Films Electrodeposited from Aqueous Solutions, *Z. Phys. Chem.*, 2016, **9**, 1281–1302.

36 M. A. Kamensky, S. N. Eliseeva, G. Láng, M. Ujvári and V. V. Kondratiev, Electrochemical Properties of Overoxidized Poly-3,4-Ethylenedioxythiophene, *Russ. J. Electrochem.*, 2018, **54**, 893–901, DOI: 10.1134/S1023193518130219.

37 K. Sun, S. Zhang, P. Li, Y. Xia, X. Zhang, D. Du, F. H. Isikgor and J. Ouyang, Review on Application of PEDOTs and PEDOT:PSS in Energy Conversion and Storage Devices, *J. Mater. Sci.: Mater. Electron.*, 2015, **26**, 4438–4462, DOI: 10.1007/s10854-015-2895-5.

38 L. Stepien, A. Roch, R. Tkachov, B. Leupolt, L. Han, N. van Ngo and C. Leyens, Thermal Operating Window for PEDOT:PSS Films and Its Related Thermoelectric Properties, *Synth. Met.*, 2017, **225**, 49–54, DOI: 10.1016/j.synthmet.2016.11.017.

39 H. Shi, C. Liu, Q. Jiang and J. Xu, Effective Approaches to Improve the Electrical Conductivity of PEDOT:PSS: A Review, *Adv. Electron. Mater.*, 2015, **1**, 1500017, DOI: 10.1002/aelm.201500017.

40 Q. Wei, M. Mukaida, W. Ding and T. Ishida, Humidity Control in a Closed System Utilizing Conducting Polymers, *RSC Adv.*, 2018, **8**, 12540–12546, DOI: 10.1039/C8RA01776J.

41 L. Zhanshayeva, V. Favaron and G. Lubineau, Macroscopic Modeling of Water Uptake Behavior of PEDOT:PSS Films, *ACS Omega*, 2019, **4**, 21883–21890, DOI: 10.1021/ACSOMEGA.9B02866/ASSET/IMAGES/LARGE/AO9B02866_0006.JPEG.

42 H. S. Park, S. J. Ko, J. S. Park, J. Y. Kim and H. K. Song, Redox-Active Charge Carriers of Conducting Polymers as a Tuner of Conductivity and Its Potential Window, *Sci. Rep.*, 2013, **3**, 2454, DOI: 10.1038/srep02454.

43 Z. Fan, D. Du, H. Yao and J. Ouyang, Higher PEDOT Molecular Weight Giving Rise to Higher Thermoelectric Property of PEDOT:PSS: A Comparative Study of Clevios P and Clevios PH1000, *ACS Appl. Mater. Interfaces*, 2017, **9**, 11732–11738, DOI: 10.1021/ACSAMI.6B15158.

44 Y. Xia and J. Ouyang, Significant Different Conductivities of the Two Grades of Poly(3,4-Ethylenedioxythiophene):Poly(Styrenesulfonate), Clevios P and Clevios PH1000, Arising from Different Molecular Weights, *ACS Appl. Mater. Interfaces*, 2012, **4**, 4131–4140, DOI: 10.1021/AM300881M.

45 R. McNeill, R. Siudak, J. Wardlaw and D. Weiss, Electronic Conduction in Polymers. I. The Chemical Structure of Polypyrrole, *Aust. J. Chem.*, 1963, **16**, 1056, DOI: 10.1071/CH9631056.

46 B. Bolto and D. Weiss, Electronic Conduction in Polymers. II. The Electrochemical Reduction of Polypyrrole at Controlled Potential, *Aust. J. Chem.*, 1963, **16**, 1076, DOI: 10.1071/CH9631076.

47 B. Bolto, R. McNeill and D. Weiss, Electronic Conduction in Polymers. III. Electronic Properties of Polypyrrole, *Aust. J. Chem.*, 1963, **16**, 1090, DOI: 10.1071/CH9631090.

48 K. Keiji Kanazawa, A. F. Diaz, W. D. Gill, P. M. Grant, G. B. Street, G. Piero Gardini and J. F. Kwak, Polypyrrole: An Electrochemically Synthesized Conducting Organic Polymer, *Synth. Met.*, 1980, **1**, 329–336, DOI: 10.1016/0379-6779(80)90022-3.

49 A. F. Diaz and J. I. Castillo, A Polymer Electrode with Variable Conductivity: Polypyrrole, *J. Chem. Soc. Chem. Commun.*, 1980, 397–398, DOI: 10.1039/c39800000397.

50 E. V. Zolotukhina, I. S. Bezverkhyy and M. A. Vorotyntsev, One-Stage Periodical Anodic-Cathodic Double Pulse Deposition of Nanocomposite Materials. Application to Prussian Blue/Polypyrrole Film Coated Electrodes, *Electrochim. Acta*, 2014, **122**, 247–258, DOI: 10.1016/j.electacta.2013.10.182.

51 P. K. Lee, P. M. Nia and P. M. Woi, Facile Self-Assembled Prussian Blue-Polypyrrole Nanocomposites on Glassy Carbon: Comparative Synthesis Methods and Its Electrocatalytic Reduction towards H2O2, *Electrochim. Acta*, 2017, **246**, 841–852, DOI: 10.1016/j.electacta.2017.06.083.

52 A. A. Karyakin and M. F. Chaplin, Polypyrrole-Prussian Blue Films with Controlled Level of Doping: Codeposition of Polypyrrole and Prussian Blue, *J. Electroanal. Chem.*, 1994, **370**, 301–303, DOI: 10.1016/0022-0728(93)03163-J.

53 Q. Xue, L. Li, Y. Huang, R. Huang, F. Wu and R. Chen, Polypyrrole-Modified Prussian Blue Cathode Material for Potassium Ion Batteries via in Situ Polymerization Coating, *ACS Appl. Mater. Interfaces*, 2019, **11**, 22339–22345, DOI: 10.1021/acsami.9b04579.

54 M. Chen, X. Li, Y. Yan, Y. Yang, Q. Xu, H. Liu and Y. Xia, Polypyrrole-Coated K2Mn[Fe(CN)6] Stabilizing Its Interfaces and Inhibiting Irreversible Phase Transition during the Zinc Storage Process in Aqueous Batteries, *ACS Appl. Mater. Interfaces*, 2022, **14**, 1092–1101, DOI: 10.1021/acsami.1c20649.

55 W. J. Li, S. L. Chou, J. Z. Wang, J. L. Wang, Q. F. Gu, H. K. Liu and S. X. Dou, Multifunctional Conducing Polymer Coated Na1+xMnFe(CN)6 Cathode for Sodium-Ion Batteries with Superior Performance via a Facile and One-Step Chemistry Approach, *Nano Energy*, 2015, **13**, 200–207, DOI: 10.1016/j.nanoen.2015.02.019.

56 A. L. Pang, A. Arsad and M. Ahmadipour, Synthesis and Factor Affecting on the Conductivity of Polypyrrole: A Short Review, *Polym. Adv. Technol.*, 2021, **32**, 1428–1454, DOI: 10.1002/PAT.5201.

57 R. Ansari, Polypyrrole Conducting Electroactive Polymers: Synthesis and Stability Studies, *J. Chem.*, 2006, **3**, 860413, DOI: 10.1155/2006/860413.

58 S. Cho, J. S. Lee and H. Joo, Recent Developments of the Solution-Processable and Highly Conductive Polyaniline Composites for Optical and Electrochemical Applications, *Polymers*, 2019, **11**, 1965, DOI: 10.3390/POLYM11121965.

59 G. Liao, Q. Li and Z. Xu, The Chemical Modification of Polyaniline with Enhanced Properties: A Review, *Prog. Org. Coat.*, 2019, **126**, 35–43, DOI: 10.1016/J.PORGCOAT.2018.10.018.

60 M. Beygisangchin, S. A. Rashid, S. Shafie, A. R. Sadrolhosseini and H. N. Lim, Preparations, Properties, and Applications of Polyaniline and Polyaniline Thin Films—a Review, *Polymers*, 2021, **13**, DOI: 10.3390/polym13122003.

61 Y. Zhang, L. Xu, H. Jiang, Y. Liu and C. Meng, Polyaniline-Expanded the Interlayer Spacing of Hydrated Vanadium Pentoxide by the Interface-Intercalation for Aqueous Rechargeable Zn-Ion Batteries, *J. Colloid Interface Sci.*, 2021, **603**, 641–650, DOI: 10.1016/j.jcis.2021.06.141.

62 Z. Feng, J. Sun, Y. Liu, H. Jiang, M. Cui, T. Hu, C. Meng and Y. Zhang, Engineering Interlayer Space of Vanadium Oxide by Pyridinesulfonic Acid-Assisted Intercalation of Polypyrrole Enables Enhanced Aqueous Zinc-Ion Storage, *ACS Appl. Mater. Interfaces*, 2021, **13**, 61154–61165, DOI: 10.1021/acsami.1c18950.

63 Y. Zhang, R. Huang, X. Wang, Z. Wang, B. Song, Y. Du, Q. Lu, X. Chen and J. Sun, Facile Large-Scale Preparation of Vanadium Pentoxide -Polypyrrole Composite for Aqueous Zinc-Ion Batteries, *J. Alloys Compd.*, 2022, **907**, 164434, DOI: 10.1016/j.jallcom.2022.164434.

64 B. Wang, S. Dai, Z. Zhu, L. Hu, Z. Su, Y. Jin, L. Xiong, J. Gao, J. Wan, Z. Li, *et al.*, A Two-Dimensional Conductive Polymer/V2O5 Composite with Rapid Zinc-Ion Storage Kinetics for High-Power Aqueous Zinc-Ion Batteries, *Nanoscale*, 2022, **14**, 12013–12021, DOI: 10.1039/d2nr03147g.

65 Y. Du, Y. Chen, M. Yang, S. Zou, X. Song, Y. Fu, J. Li, Y. Li and D. He, Poly(3,4-Ethylenedioxythiophene)-Polystyrenesulfonate-Added Layered Vanadium Oxide Cathode for High-Performance Zinc-Ion Batteries, *ACS Appl. Energy Mater.*, 2021, **4**, 14582–14589, DOI: 10.1021/acsaem.1c03209.

66 F. S. Volkov, E. G. Tolstopjatova, S. N. Eliseeva, M. A. Kamenskii, A. I. Vypritskaia, A. I. Volkov and V. V. Kondratiev, Vanadium(V) Oxide Coated by Poly(3,4-

Ethylenedioxythiophene) as Cathode for Aqueous Zinc-Ion Batteries with Improved Electrochemical Performance, *Mater. Lett.*, 2022, **308**, 131210, DOI: 10.1016/j.matlet.2021.131210.

67 W. Wang, D. He, Y. Fang, S. Wang, Z. Zhang, R. Zhao and W. Xue, Pillaring of a Conductive Polymer in Layered V2O5 Boosting Ultra-Fast Zn2+/H+ Storage in Aqueous Media, *Electrochim. Acta*, 2022, **416**, 140270, DOI: 10.1016/j.electacta.2022.140270.

68 Y. Zhang, Z. Li, M. Liu and J. Liu, Construction of Novel Polyaniline-Intercalated Hierarchical Porous V2O5 Nanobelts with Enhanced Diffusion Kinetics and Ultra-Stable Cyclability for Aqueous Zinc-Ion Batteries, *Chem. Eng. J.*, 2023, **463**, 142425, DOI: 10.1016/j.cej.2023.142425.

69 J. Sun, Y. Zhao, Y. Liu, H. Jiang, D. Chen, L. Xu, T. Hu, C. Meng and Y. Zhang, Synthesis of V2O5·nH2O Nanobelts@polyaniline Core–Shell Structures with Highly Efficient Zn2+ Storage, *J. Colloid Interface Sci.*, 2023, **633**, 923–931, DOI: 10.1016/j.jcis.2022.11.153.

70 R. Dong, T. Zhang, J. Liu, H. Li, D. Hu, X. Liu and Q. Xu, Mechanistic Insight into Polypyrrole Coating on V2O5 Cathode for Aqueous Zinc-Ion Battery, *ChemElectroChem*, 2022, **9**, e202101441, DOI: 10.1002/celc.202101441.

71 J. Kumankuma-Sarpong, W. Guo and Y. Fu, Yttrium Vanadium Oxide–Poly(3,4-Ethylenedioxythiophene) Composite Cathode Material for Aqueous Zinc-Ion Batteries, *Small Methods*, 2021, **5**, 2100544, DOI: 10.1002/smtd.202100544.

72 S. Li, X. Wei, C. Wu, B. Zhang, S. Wu and Z. Lin, Constructing Three-Dimensional Structured V2O5/Conductive Polymer Composite with Fast Ion/Electron Transfer Kinetics for Aqueous Zinc-Ion Battery, *ACS Appl. Energy Mater.*, 2021, **4**, 4208–4216, DOI: 10.1021/acsaem.1c00573.

73 Z. Feng, J. Sun, Y. Liu, H. Jiang, T. Hu, M. Cui, F. Tian, C. Meng and Y. Zhang, Polypyrrole-Intercalation Tuning Lamellar Structure of V2O5·nH2O Boosts Fast Zinc-Ion Kinetics for Aqueous Zinc-Ion Battery, *J. Power Sources*, 2022, **536**, 231489, DOI: 10.1016/j.jpowsour.2022.231489.

74 Q. Sun, L. Chang, Y. Liu, W. Nie, T. Duan, Q. Xu, H. Cheng and X. Lu, Chrysanthemum-like Polyaniline-Anchored PANI0.22·V2O5·0.88H2O-Hybridized Cathode for High-Stable Aqueous Zinc-Ion Batteries, *ACS Appl. Energy Mater.*, 2023, **6**, 3102–3112, DOI: 10.1021/acsaem.3c00063.

75 J. Huang, X. Tang, K. Liu, G. Fang, Z. He and Z. Li, Interfacial Chemical Binding and Improved Kinetics Assisting Stable Aqueous Zn–MnO2 Batteries, *Mater. Today Energy*, 2020, **17**, 100475, DOI: 10.1016/j.mtener.2020.100475.

76 P. Ruan, X. Xu, X. Gao, J. Feng, L. Yu, Y. Cai, X. Gao, W. Shi, F. Wu, W. Liu, *et al.*, Achieving Long-Cycle-Life Zn-Ion Batteries through Interfacial Engineering of MnO2-Polyaniline Hybrid Networks, *Sustainable Mater. Technol.*, 2021, **28**, e00254, DOI: 10.1016/j.susmat.2021.e00254.

77 X. Liao, C. Pan, Y. Pan and C. Yin, Synthesis of Three-Dimensional β-MnO2/PPy Composite for High-Performance Cathode in Zinc-Ion Batteries, *J. Alloys Compd.*, 2021, **888**, 161619, DOI: 10.1016/j.jallcom.2021.161619.

78 H. Chen, W. Ma, J. Guo, J. Xiong, F. Hou, W. Si, Z. Sang and D. Yang, PEDOT-Intercalated MnO2 Layers as a High-Performance Cathode Material for Aqueous Zn-Ion Batteries, *J. Alloys Compd.*, 2023, **932**, 167688, DOI: 10.1016/j.jallcom.2022.167688.

79 L. Wang, X. Wang, B. Song, Z. Wang, L. Zhang and Q. Lu, Facile in Situ Synthesis of PEDOT Conductor Interface at the Surface of MnO2 Cathodes for Enhanced Aqueous Zinc-Ion Batteries, *Surf. Interfaces*, 2022, **33**, 102222, DOI: 10.1016/j.surfin.2022.102222.

80 M. A. Kamenskii, F. S. Volkov, S. N. Eliseeva, R. Holze and V. V. Kondratiev, Comparative Study of PEDOT- and PEDOT:PSS Modified δ-MnO 2 Cathodes for Aqueous Zinc Batteries with Enhanced Properties, *J. Electrochem. Soc.*, 2023, **170**, 010505, DOI: 10.1149/1945-7111/acabec.

81 J. Mao, F. F. Wu, W. H. Shi, W. X. Liu, X. L. Xu, G. F. Cai, Y. W. Li and X. H. Cao, Preparation of Polyaniline-Coated Composite Aerogel of MnO2 and Reduced Graphene Oxide for High-Performance Zinc-Ion Battery, *Chin. J. Polym. Sci.*, 2020, **38**, 514–521, DOI: 10.1007/s10118-020-2353-6.

82 T. Niu, J. Li, Y. Qi, X. Huang and Y. Ren, Preparation and Electrochemical Properties of α-MnO2/RGO-PPy Composite as Cathode Material for Zinc-Ion Battery, *J. Mater. Sci.*, 2021, **56**, 16582–16590, DOI: 10.1007/s10853-021-06266-6.

83 Y. Zhang, G. Xu, X. Liu, X. Wei, J. Cao and L. Yang, Scalable In Situ Reactive Assembly of Polypyrrole-Coated MnO2 Nanowire and Carbon Nanotube Composite as Freestanding Cathodes for High Performance Aqueous Zn-Ion Batteries, *ChemElectroChem*, 2020, **7**, 2762–2770, DOI: 10.1002/celc.202000253.

84 J. W. Xu, Q. L. Gao, Y. M. Xia, X. S. Lin, W. L. Liu, M. M. Ren, F. G. Kong, S. J. Wang and C. Lin, High-Performance Reversible Aqueous Zinc-Ion Battery Based on Iron-Doped Alpha-Manganese Dioxide Coated by Polypyrrole, *J. Colloid Interface Sci.*, 2021, **598**, 419–429, DOI: 10.1016/j.jcis.2021.04.057.

85 M. Baghodrat, G. Zampardi, J. Glenneberg and F. La Mantia, Influence of the Thermal Treatment on the Structure and Cycle Life of Copper Hexacyanoferrate for Aqueous Zinc-Ion Batteries, *Batteries*, 2023, **9**, 170, DOI: 10.3390/batteries9030170.

86 G. Zampardi, M. Warnecke, M. Tribbia, J. Glenneberg, C. Santos and F. La Mantia, Effect of the Reactants Concentration on the Synthesis and Cycle Life of Copper Hexacyanoferrate for Aqueous Zn-Ion Batteries, *Electrochem. Commun.*, 2021, **126**, 107030, DOI: 10.1016/J.ELECOM.2021.107030.

87 M. Baghodrat, J. Glenneberg, G. Zampardi and F. La Mantia, Harnessing the Benefits of PEDOT : PSS Conductive Coating for Prolonged Cycle Life of Copper Hexacyanoferrate in Aqueous Zinc-Ion Batteries, *Batteries Supercaps*, 2024, **7**, e202400156, DOI: 10.1002/batt.202400156.

88 P. P. Puthiyaveetil, A. Nair, S. Dilwale, M. Kurian, K. Joshi and S. Kurungot, Insights on Prussian Blue Analogue Cathode Material Engineered with Polypyrrole Surface Protection Layer for Aqueous Rechargeable Zinc Metal Battery, *Small*, 2024, 2409947, DOI: 10.1002/smll.202409947.

89 Q. Liu, Z. Ma, Z. Chen, M. Cui, H. Lei, J. Wang, J. B. Fei, N. He, Y. Liu, Q. Liu, *et al.*, A Polyaniline Surface-Modified Prussian Blue Analogue Cathode for Flexible Aqueous Zn-Ion Batteries, *Chem. Commun.*, 2022, **58**, 8226–8229, DOI: 10.1039/d2cc02724k.

90 H. C. Hesse, M. Schimpe, D. Kucevic and A. Jossen, Lithium-Ion Battery Storage for the Grid - A Review of Stationary Battery Storage System Design Tailored for Applications in Modern Power Grids, *Energies*, 2017, **10**, 2107, DOI: 10.3390/en10122107.

91 G. Zampardi and F. La Mantia, Open Challenges and Good Experimental Practices in the Research Field of Aqueous Zn-Ion Batteries, *Nat. Commun.*, 2022, **13**, 687, DOI: 10.1038/s41467-022-28381-x.

92 Z. Lin, T. Liu, X. Ai and C. Liang, Aligning Academia and Industry for Unified Battery Performance Metrics, *Nat. Commun.*, 2018, **9**, 1–5, DOI: 10.1038/s41467-018-07599-8.

93 Y. Liu, T. Wang, Y. Sun, M. Zhang, G. Gao, J. Yang and K. Cai, Fast and Efficient In-Situ Construction of Low Crystalline PEDOT-Intercalated V2O5 Nanosheets for High-Performance Zinc-Ion Battery, *Chem. Eng. J.*, 2024, **484**, 149501, DOI: 10.1016/j.cej.2024.149501.

94 T. Yang, D. Xin, N. Zhang, J. Li, X. Zhang, L. Dang, Q. Li, J. Sun, X. He, R. Jiang, *et al.*, Interfacial Polymerization of PEDOT Sheath on V2O5 Nanowires for Stable Aqueous Zinc Ion Storage, *J. Mater. Chem. A*, 2024, **12**, 10137–10147, DOI: 10.1039/d4ta01136h.

95 X. Yin, X. Wu, F. Liu and B. Long, PEDOT-Coated VOOH Nanoparticles as a High-Capacity Cathode for Aqueous Zinc-Ion Battery, *J. Electroanal. Chem.*, 2024, **972**, 118614, DOI: 10.1016/j.jelechem.2024.118614.

96 S. Ye, S. Sheng, Y. Wang, J. Li, Q. Li, L. Meng, Q. Chen and H. Yao, Synthesis of Binder-Free Hydrated Vanadium Oxide-Polyaniline Electrodes via in Situ Polymerization for High-Performance Aqueous Zinc-Ion Batteries, *Inorg. Chem. Commun.*, 2024, **166**, 112656, DOI: 10.1016/j.inoche.2024.112656.

97 P. He, R. Yuan, B. Wang, W. Ai, M. Li, D. Xie and K. Wang, In Situ Prepared Amorphous VOH-Polyaniline@Carbon Cloth as Cathodes for High Performance Zinc Ion Batteries, *J. Electroanal. Chem.*, 2024, **954**, 118008, DOI: 10.1016/j.jelechem.2023.118008.

98 Y. Ruan, L. Chen, L. Cui and Q. An, PPy-Modified Prussian Blue Cathode Materials for Low-Cost and Cycling-Stable Aqueous Zinc-Based Hybrid Battery, *Coatings*, 2022, **12**, 779, DOI: 10.3390/coatings12060779.

99 P. Luo, G. Yu, W. Zhang, H. Tang, D. Zhu, F. Chao, W. Zhong, S. Dong and Q. An, "Triple-Synergistic Effect" of K+ and PANI Co-Intercalation Enabling the High-Rate Capability and Stability of V2O5 for Aqueous Zinc-Ion Batteries, *J. Colloid Interface Sci.*, 2024, **659**, 267–275, DOI: 10.1016/j.jcis.2023.12.167.

100 S. Mao, Y. Wu, S. Xu, T. Xiao, Y. Li, Z. Li, X. Pan, B. Yuan, Y. Xu, H. Wen, *et al.*, Design of Large-Spacing, High-Stability PANI-NixV2O5 Nanobelts as Cathode for Aqueous Zinc-Ion Batteries Using an Organic-Inorganic Co-Embedding Strategy, *J. Power Sources*, 2025, **628**, 235912, DOI: 10.1016/j.jpowsour.2024.235912.

101 Y. Li, B. Liu, J. Ding, X. Han, Y. Deng, T. Wu, K. Amine, W. Hu, C. Zhong and J. Lu, Understanding the Gap between Academic Research and Industrial Requirements in Rechargeable Zinc-Ion Batteries, *Batteries Supercaps*, 2021, **4**, 60–71, DOI: 10.1002/batt.202000124.